






Article

Lab-Scale Study of Temperature and Duration Effects on Carbonized Solid Fuels Properties Produced from Municipal Solid Waste Components

Kacper Świechowski ¹, Paweł Stępień ², Ewa Syguła ^{1,*}, Jacek A. Koziel ³ and Andrzej Białowiec ^{1,3,*}

¹ Department of Applied Bioeconomy, Wrocław University of Environmental and Life Sciences, 37/41 Chełmońskiego Str., 51-630 Wrocław, Poland; kacper.swiechowski@upwr.edu.pl

² Institute of Agricultural Engineering, Wrocław University of Environmental and Life Sciences, 37/41 Chełmońskiego Str., 51-630 Wrocław, Poland; pawel.stepien@upwr.edu.pl

³ Department of Agricultural and Biosystems Engineering, Iowa State University, Ames, IA 50011, USA; koziel@iastate.edu

* Correspondence: ewa.syguła@upwr.edu.pl (E.S.); andrzej.bialowiec@upwr.edu.pl (A.B.)

Abstract: In work, data from carbonization of the eight main municipal solid waste components (carton, fabric, kitchen waste, paper, plastic, rubber, paper/aluminum/polyethylene (PAP/AL/PE) composite packaging pack, wood) carbonized at 300–500 °C for 20–60 min were used to build regression models to predict the biochar properties (proximate and ultimate analysis) for particular components. These models were then combined in general models that predict the properties of char made from mixed waste components depending on pyrolysis temperature, residence time, and share of municipal solid waste components. Next, the general models were compared with experimental data (two mixtures made from the above-mentioned components carbonized at the same conditions). The comparison showed that most of the proposed general models had a determination coefficient (R^2) over 0.6, and the best prediction was found for the prediction of biochar mass yield ($R^2 = 0.9$). All models were implemented into a spreadsheet to provide a simple tool to determine the potential of carbonization of municipal solid waste/refuse solid fuel based on a local mix of major components.

Keywords: CO₂-assisted pyrolysis; organic waste; waste conversion; thermal treatment; waste to energy; waste to carbon; regression models; waste recycling; municipal waste; circular economy



Citation: Świechowski, K.; Stępień, P.; Syguła, E.; Koziel, J.A.; Białowiec, A. Lab-Scale Study of Temperature and Duration Effects on Carbonized Solid Fuels Properties Produced from Municipal Solid Waste Components. *Materials* **2021**, *14*, 1191. <https://doi.org/10.3390/ma14051191>

Academic Editor: Jon Alvarez

Received: 30 January 2021

Accepted: 25 February 2021

Published: 3 March 2021

Publisher's Note: MDPI stays neutral with regard to jurisdictional claims in published maps and institutional affiliations.



Copyright: © 2021 by the authors. Licensee MDPI, Basel, Switzerland. This article is an open access article distributed under the terms and conditions of the Creative Commons Attribution (CC BY) license (<https://creativecommons.org/licenses/by/4.0/>).

1. Introduction

Waste generation is an inherent element of human activity and economic development. The Organization for Economic Co-Operation and Development (OECD) estimates increases in waste production by 0.69% for each 1% of the gross domestic product (GDP) [1]. Proper municipal solid waste (MSW) management becomes more difficult every year as new materials and products are introduced. For example, new packing materials are increasingly composite materials (the mixture of several materials designed for desired properties). Composite waste materials are challenging to effectively recycle when the mechanical separation is applied [2]. Thus, new technologies are needed to sustainably treat MSW in the context of zero landfilling and circular economy goals.

The MSW is a heterogeneous mixture of various materials generated in households, public, commercial and industrial sectors [3]. Many factors affect the MSW composition (e.g., economic development, the level and type of urbanization, culture, law, climate, season, environmental awareness of citizens). The MSW composition is highly variable with time, but in general, organic waste constitutes up to 83% [4]. The principal organic components of MSW are food waste, green waste (e.g., grass clippings, leaves, branches), wood, paper, carton, rubber, and the most abundant plastics [5]. In the last 20 years, plastics production doubled to ~335,000,000 Mg globally and is estimated to exceed >600,000,000 Mg in the next ten years [6].

The EU Directive 2008/98/EC proposed the waste management hierarchy, promoting waste prevention, followed by reuse, and then recycling [7]. If recycling is not possible, the recovery should be used (e.g., incineration with energy recovery), and finally, residual waste disposal [7]. The Circular Economic Action Plan has recently been adopted by the European Commission, aiming at climate neutrality by 2050. One of the targets is to use waste instead of raw materials [8].

To date, a common practice in the EU is the initial separation of MSW fractions directly at the source (e.g., separation of paper, plastic, biodegradable waste, glass, and residual waste at households). After collection, these pre-separated fractions are processed in a waste mechanical sorting plant. The residual wastes usually are treated in so-called mechanical biological treatment plants (MBT) [9,10]. The main goals are to (i) recycle high-value materials, (ii) to produce refuse-derived fuel (RDF) from waste that cannot be recycled, (iii), and to stabilize biodegradable waste before its disposal in landfills [11].

RDF is a fuel made from various types of materials by its homogenization (shredding and mixing), removal of not flammable waste (e.g., glasses, metals, stones), removal of chlorinated waste, and drying if needed (e.g., by bio-drying). The RDFs are used for heat and electricity production in specially designed incineration plants or in cement kilns to substitute fossil fuels. RDF has to meet standards that depend on user requirements. More valuable RDF has a higher calorific value, lower ash content, and moisture. RDF fuel quality can be improved by mechanical treatment. However, the thermal conversion of RDFs is growing [12–14].

The thermal conversion of waste in the absence or limited amount of oxygen includes torrefaction, hydrothermal carbonization, low-temperature pyrolysis, pyrolysis (slow, intermediate, fast), and gasification. Torrefaction and low-temperature pyrolysis are favorable means to upgrade the RDF quality, as these processes lead to a significant increase of carbonized solid fuel (CSF) calorific values [15,16]. The higher temperatures (e.g., pyrolysis at ~600 °C) leads to the increased production of gases and liquid fractions at the expense of solid fraction and the ultimate loss of the CSF's calorific value [14,17,18].

The preferred low-temperature pyrolysis occurs at 300–550 °C and results in biochars (e.g., CSF when RDF is a feedstock) and pyrolysis gases, from which the liquid fraction can be separated [19]. The CSF mainly consists of carbon. The pyrolytic gas consists of H₂, CO, CO₂, CH₄, and other low-molecular-weight hydrocarbon gases, whereas the liquid fractions are a mixture of various oils that can be processed into useful chemicals. There is also possible to use pyrolysis gases (with or without liquid separation) to provide energy to the pyrolysis process by its incineration. The optimal temperature, heating rate, process duration, and size of particles depend on the processed material and its processing goals. For CSF production, a relatively slow heating rate is recommended [20,21].

Mass yield (MY), energy densification ratio (EDr), and energy yield (EY) are the key parameters characterizing the production of CSF for energy purposes. The mass yield shows how much CSF will be obtained after pyrolysis in relation to the initial mass. The energy densification ratio describes how much energy was densified in CSF in relation to the calorific value of the feedstock. The energy yield is the amount of energy remaining in the material after processing and is given in %.

Proximate analyses such as moisture content (MC), volatile matter content (VM), fixed carbon content (FC), and ash content (AC) are useful for fuels ($MC + VM + FC + AC = 100\%$) [22,23]. The combustible parts (CP) and volatile solids (VS) are often reported for waste pyrolysis. The CP is determined mainly for MSW (as all organic and inorganic matter that is converted into gas during incineration at 815 °C) [24]. The VS (a.k.a. organic matter content/loss on ignition) consists of organic substances converted into a gas at 550 °C [25]. The calorific value determination is focused on the high heating value (HHV) and low heating value (LHV), wherein typically, the LHV is calculated as a function of HHV, MC, and H content [26].

For the ultimate analysis, the elemental composition is determined (C, H, N, S, and O), where (typically) $C + H + N + S + O + AC + MC = 100\%$ [22]. In general, the higher the C and H content, the higher the calorific value. After pyrolysis, most of the carbon stays in

CSF, whereas most of the H goes to the gaseous phase. O decreases the calorific value, and N and S are a source of combustion pollutants (NO_x and SO_x) [27].

The inherent variability in MSW composition is the most significant barrier to determining the resulting CSF fuel properties [28]. Each time the raw feedstock material has to be tested, it could be time-consuming and costly. Thus, to minimize resources, methods are used to predict the test material's properties under different process conditions [29]. Process and biochar properties modeling can be done using data from elemental composition, proximate analysis, or other analyses, which correlate to modeled variables. This modeling can be done using mathematical models (empirical, based on implicit theory, semiempirical, or neural networks). The most commonly used are linear regression models, where empirical data is subjected to regression by the least-squares method. The most well-known regression model is used for HHV determination and is called Dulong's formula [30]. There are also other formulas for different materials [29] and different input data [31]. The precision of equations based on proximate analysis is lower than that of CHNS or neural network analysis, but the main advantage of these methods is their simple structure and low cost [32].

In this work, we used different approaches to modeling of pyrolysis process and biochar properties. We used experimental data from processed materials and correlated it with process conditions. Conventional modeling uses data from substrate analysis (proximate, ultimate, other) and then correlates it with modeled variable. As a result, our models do not require time-consuming and costly analyses of substrates as input data.

The objective of this work was to develop empirical models for the CSF quality that incorporate the effects of low-temperature pyrolysis conditions (duration (t), temperature (T) for the mixture of the main constituents of MSW. The work's main result was a calculation tool (Excel-based file for modeling) that predicts CSF properties from waste pyrolyzed at 300–500 °C at durations up to 60 min without the need to analyze input material characteristics.

2. Materials and Methods

The quantified parameters included MY, EDr, EY, MC, OM, AC, CP, and C, H, N, and S content. The main MSW components included: carton, fabric (cotton t-shirt), kitchen waste, paper, plastic, rubber, paper/aluminum/polyethylene (PAP/AL/PE) composite packaging packs, and wood. A detailed description of methods is provided elsewhere [14]. 'CSF' replaces the name 'biochar' used for the thermally processed material in similar conditions for the rest of the manuscript.

First, measured properties of particular waste components were subjected to four regression models (models I–IV). The best-fitted model was chosen for each parameter and each waste component among these four models, based on the determination coefficients (R^2) and Akaike information criterion (AIC). Then, the best-fitted models for particular waste and parameters were combined in one general model. Overall, 11 general models were developed, one for each studied parameter. Next, the general models were compared with experimental data. The experimental data included two (example) RDF mixtures (with a known share of particular components) carbonized at the same condition conditions as the individual components.

2.1. Materials

The main MSW components were: carton (grey carton), fabric (cotton t-shirt), kitchen waste (vegetables, 41.6% (carrot 13.86%, potato 13.86%, salad 13.86%); banana peel, 29.7%; basic food (pasta 7.43%, rice 7.43%, bread 7.43%); chicken, 0.2%; eggshells, 4%; and walnut shells, 2.2% by weight), paper (office paper), plastic (polyethylene foil), rubber (car inner tube), PAP/AL/PE composite packaging pack (Tetra Pak, Lund, Sweden, Lausanne, Switzerland), and wood (pruning tree branches).

The RDF mixtures were used for validation of the general models. The mixture consisted of the following fractions: RDF—carton, 9.64%; fabric, 6.20%; kitchen waste,

4.02%; paper, 9.64%; plastic, 34.23%; rubber, 9.6%; PAP/AL/PE composite packaging pack, 12.22%; wood, 14.45%; RDF 2—carton, 8.57%; fabric, 9.54%; kitchen waste, 7.10%; paper, 8.57%; plastic, 45.24%; rubber, 7.71%; PAP/AL/PE composite packaging pack, 5.81%; wood, 7.46%. More detailed information is presented elsewhere [14].

2.2. Methods

2.2.1. Low-Temperature Pyrolysis

Each main component and RDF mixtures were carbonized at 300–500 °C (interval 20 °C, and residence time 20–60 min (interval 20 min) using a muffle furnace (Snol 8.1/1100, Utena, Lithuania). CO₂ was supplied (2.5 dm³·min⁻¹) to provide inert conditions. Samples were heated at 50 °C·min⁻¹ to the setpoint temperature. After the end of setpoint residence time (20–60 min), the furnace was cooled down by itself while the CO₂ was still provided to prevent the self-ignition of carbonized solid fuels. The CSF samples were then removed from the furnace when the temperature was <200 °C [14].

2.2.2. Regression Modeling

Raw data used for the regression model come from previous work [14]. In short, for each produced CSF analyzed for MY, EDr, EY, C, H, N, and S content, 1 repetition was done; whereas, for MC, OM, AC, and CP, three repetitions were completed. Therefore, models of MY, EDr, EY, C, H, N, and S for each material was made using 33 measurement points, whereas MC, OM, AC, and CP were made using 99 measurement points.

Properties of each waste component were subjected to four regression models using the method of least squares to estimate intercept (a_1) and regression coefficients (a_2 – a_6):

- Model I—linear equation $y(T,t) = a_1 + a_2T + a_3 \times t$;
- Model II—second-order polynomial equation $y(T,t) = a_1 + a_2 \times T + a_3 \times T^2 + a_4 \times t + a_5 \times t^2$;
- Model III—factorial regression equation $y(T,t) = a_1 + a_2 \times T + a_3 \times t + a_4 \times T \times t$;
- Model IV—response surface regression equation $y(T,t) = a_1 + a_2 \times T + a_3 \times t + a_4 \times T^2 + a_5 \times t^2 + a_6 \times T \times t$.

where:

$y(T,t)$ —the variable that depends on process temperature and time.

T —low-temperature pyrolysis process temperature (°C), (300–500 °C).

t —low-temperature pyrolysis process residence time (min) (20–60 min).

a_1 —intercept

a_2 – a_6 —regression coefficients

The best-fitted model was chosen for each parameter and each waste component among models I–IV, using R^2 and AIC, respectively [33].

$$R^2 = \frac{\sum_{i=1}^n (\hat{y}_i - \bar{y})^2}{\sum_{i=1}^n (y_i - \bar{y})^2} \quad (1)$$

where:

R^2 —determination coefficient;

i —repeated observations;

\hat{y}_i —value of the dependent variable predicted by the regression model;

\bar{y} —mean value of the dependent variable (measured);

y_i —value of the dependent variable (measured).

$$AIC = n \cdot \ln\left(\sum_{i=1}^n e_i^2\right) + 2 \cdot K \quad (2)$$

where:

AIC—a value of Akaike analysis;

n—the number of measurements;
 e—the value of the residuals of the model (defined as the difference between predicted and experimental value);
 K—number of regressions coefficients (including the intercept).

The $a_1, a_2-a_6,$ and R^2 were calculated using StatSoft software Statistica 13.3 (TIBCO Software Inc., Palo Alto, CA, USA). The best-fitting model for each variable was determined as follows. First, the model (I–IV) with the highest R^2 was chosen. If several models had similar R^2 , the model with the lowest AIC was chosen as the best-fitted. The R^2 quantifies how well models match to data, whereas the AIC points to the simpler model with similar matching.

2.2.3. General Model

The best-fitted models for each main waste and parameters were combined into one general model:

$$y_{CSF}(T, t) = \frac{\sum_i^n (y_i(T, t) \cdot \%share_i)}{\sum_i^n (\%share_i)} \tag{3}$$

where:

$y_{CSF}(T, t)$ —the estimated value of the studied parameter of CSF from a mixture of MSW/RDF at T & t conditions, MJ·kg⁻¹;

$y_i(T, t)$ —the estimated value of the studied parameter of i-CSF from individual MSW/RDF component under T & t conditions, MJ·kg⁻¹;

$\%share_i$ —percentage mass share of i-CSF from individual MSW/RDF component in the total mass of CSF from MSW/RDF mixture, %.

Overall, 11 general models were developed, one for each studied parameter. Next, general models were compared with experimental data of two RDF mixtures (with a known share of particular components) carbonized at the same condition conditions as the individual components, RDF 1 and RDF 2. A linear correlation (R) and R^2 were used to compare general models.

3. Results and Discussion

3.1. Regression Models

3.1.1. Mass Yield of CSF

For all MY models (except rubber), model IV had the highest R^2 and the lowest AIC; therefore, model IV was assumed as the best fit. The best model for rubber was model II (Table A1 in Appendix A). The influence of low-temperature pyrolysis temperature and residence time on CSF's mass yield of best-fit equations are shown in Table 1.

Table 1. The chosen (best-fitted) mathematical models of the influence of the pyrolysis temperature and residence time on the mass yield of carbonized solid fuel (CSF) produced from different refuse-derived fuel (RDF) components.

Material	Equation	R ²
Carton	$MY(T,t) = 453.833 - 1.49491 \times T - 3.47577 \times t + 0.00137504 \times T^2 + 0.0133644 \times t^2 + 0.00499467 \times T \times t$	0.77
Fabric	$MY(T,t) = 661.088 - 2.36376 \times T - 4.65892 \times t + 0.00223887 \times T^2 + 0.0187874 \times t^2 + 0.00669526 \times T \times t$	0.78
Kitchen waste	$MY(T,t) = 337.338 - 1.1419 \times T - 1.70984 \times t + 0.00109174 \times T^2 + 0.00214157 \times t^2 + 0.00324575 \times T \times t$	0.85
Paper	$MY(T,t) = 395.322 - 1.30458 \times T - 2.76693 \times t + 0.00120622 \times T^2 + 0.0079086 \times t^2 + 0.00453242 \times T \times t$	0.79
Plastic	$MY(T,t) = -390.144 + 2.47977 \times T + 2.62558 \times t - 0.00295447 \times T^2 + 0.0075406 \times t^2 - 0.00959024 \times T \times t$	0.72
Rubber	$MY(T,t) = 216.783 - 0.27841 \times T - 5.73357 \cdot 10^{-5} \times T^2 - 0.961876 \times t + 0.00652372 \times t^2$	0.85
PAP/AL/PE composite packaging pack	$MY(T,t) = 268.722 - 0.611037 \times T - 1.96903 \times t + 0.000373715 \times T^2 + 0.0131861 \times t^2 + 0.00132244 \times T \times t$	0.83
Wood	$MY(T,t) = 341.093 - 1.08665 \times T - 2.14508 \times t + 0.000978011 \times T^2 + 0.00776588 \times t^2 + 0.00316288 \times T \times t$	0.81

The MY of the CSF from the carton decreased with increasing T and t from 92% to 32%, model $R^2 = 0.77$. The CSF results from the fabric showed that as the T increased, the MY decreased from 98% to 18%, model $R^2 = 0.78$. The MY of the CSF from kitchen waste decreased with increasing T and t from 85% to 37%, the model $R^2 = 0.85$. The paper pyrolysis results showed that as the T and t increase, the MY decreased from 91% to 37%, model $R^2 = 0.79$. The plastic subjected to the pyrolysis was characterized by a high drop in MY with an increase in T (up to 500 °C) and t (up to 60 min) from 99.9% to 8%, model $R^2 = 0.72$. Rubber was characterized by a linear decrease in MY with an increase in T. The increase in t did not show a significant influence on MY. The MY of CSF from rubber decreased from 99% to 40%, model $R^2 = 0.85$. The MY of the pyrolyzed PAP/AL/PE was characterized by a linear decrease with increasing T from 96% to 25%, model $R^2 = 0.85$. Wood waste was characterized by decreased MY with increasing T from 92% to 32%, model $R^2 = 0.81$.

Each material was characterized by a decreasing MY trend caused by increasing T and t. In general, the proposed models had a high R of ~0.80. The lowest R^2 was found for plastic due to outliers at 500 °C at 60 min. These outliers are probably a result of the lack of secondary reactions. The plastic (polyethylene) was pyrolyzed in the muffle furnace with the constant inert gas flow (CO_2). Therefore, the vaporized liquids were removed from the reactor. As a result, these liquids could not generate biochar in the secondary reactions that occur at >440 °C and >90 min [34].

The correlation between the experiment results and the model data for MY is shown in Figure 1. The confidence interval for correlation was 95% (dotted lines). The results showed that the proposed general model had correlations of 95% with the experimental data for RDF 1 and RDF 2, respectively. Obtained results indicate that the proposed model concerning pyrolysis' T, t, and knowledge of RDF composition could be useful to predict the MY produced from pyrolyzed RDF.

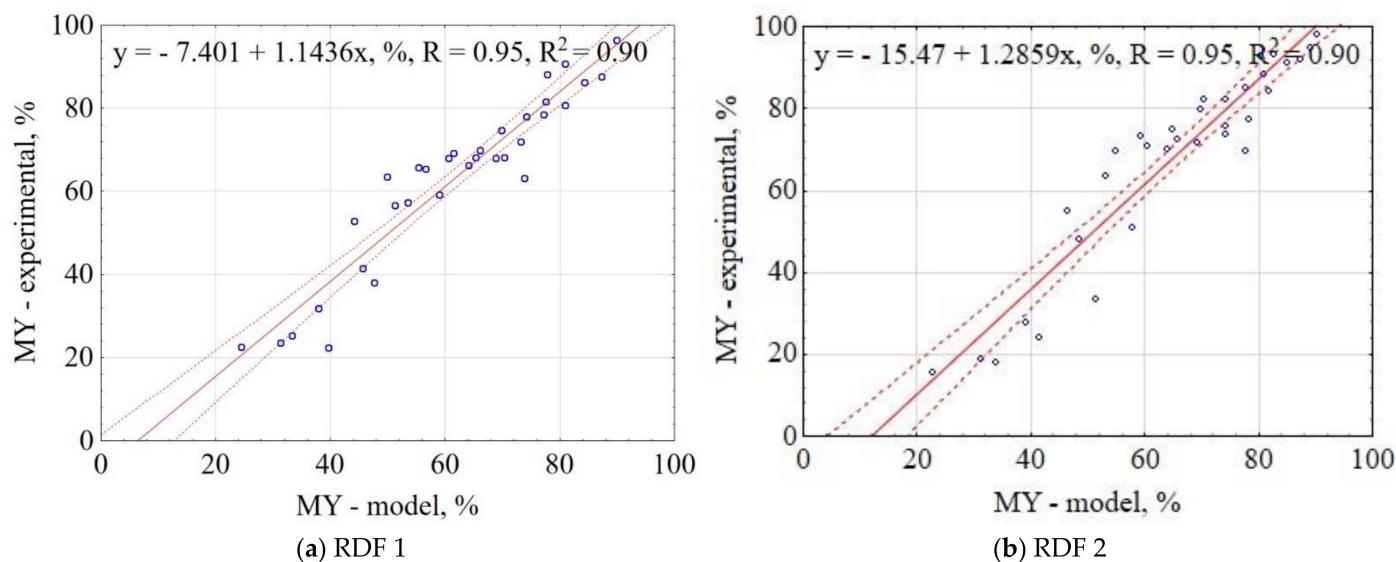


Figure 1. Correlation between experimental and estimated mass yield (MY) of carbonized RDF blends, (a) RDF 1, (b) RDF 2. Blue circles indicate the experimental and predicted data.

3.1.2. Energy Densification Ratio of CSF

For all materials, the influence of low-temperature pyrolysis T and t on EDr of CSF was best described by model IV, which had the highest R^2 and the lowest AIC (Table A1). These models' equations were summarized in Table 2.

Table 2. The chosen (best-fitted) mathematical models of the influence of the pyrolysis temperature and residence time on the energy densification ratio (EDr) of CSF produced from different RDF components.

Material	Equation	R ²
Carton	$EDr(T,t) = 0.521138 + 0.0024532 \times T + 0.00542369 \times t - 3.07672 \times 10^{-6} \times T^2 - 8.29299 \times 10^{-5} \times t^2 + 2.76737 \times 10^{-6} \times T \times t$	0.16
Fabric	$EDr(T,t) = -0.00672325 + 0.00222108 \times T + 0.0223182 \times t + 1.32688 \times 10^{-6} \times T^2 - 0.000176585 \times t^2 - 1.9214 \times 10^{-5} \times T \times t$	0.55
Kitchen waste	$EDr(T,t) = 0.119321 + 0.00462755 \times T + 0.00777896 \times t - 4.13357 \cdot 10^{-6} \times T^2 + 3.05844 \cdot 10^{-5} \times t^2 - 2.39844 \cdot 10^{-5} \times T \times t$	0.55
Paper	$EDr(T,t) = 1.9716 - 0.00364838 \times T - 0.00723548 \times t + 3.79197 \times 10^{-6} \times T^2 + 6.59619 \cdot 10^{-5} \times t^2 + 2.2538 \times 10^{-6} \times T \times t$	0.41
Plastic	$EDr(T,t) = -2.65302 + 0.0183674 \times T + 0.0136888 \times t - 2.16719 \times 10^{-5} \times T^2 + 9.6406 \cdot 10^{-5} \times t^2 - 6.10462 \times 10^{-5} \times T \times t$	0.57
Rubber	$EDr(T,t) = 0.862326 + 0.00302199 \times T - 0.00264502 \times t - 5.80671 \cdot 10^{-6} \times T^2 + 0.000101288 \times t^2 - 2.56826 \times 10^{-5} \times T \times t$	0.88
PAP/AL/PE composite packaging pack	$EDr(T,t) = -5.71804 + 0.0327167 \times T + 0.0298075 \times t - 3.66779 \times 10^{-5} \times T^2 + 2.0243 \times 10^{-5} \times t^2 - 8.0066 \times 10^{-5} \times T \times t$	0.73
Wood	$EDr(T,t) = 0.0728126 + 0.0040324 \times T + 0.00837479 \times t - 2.97147 \times 10^{-6} \times T^2 - 2.61616 \times 10^{-5} \times t^2 - 1.17289 \times 10^{-5} \times T \times t$	0.82

The EDr of CSF produced from the carton did not increase significantly with the T and t and the best-fitted model had R² = 0.16 (Table 2). The CSF produced from cotton was characterized by increasing EDr as the T increased, and the best-fitted model had R² = 0.55 (Table 2). The EDr of CSF produced from kitchen waste did not increase significantly when the process T and t increased, and the determination coefficient for the best-fitted model was R² = 0.55. The CSF produced in the paper was characterized by a decrease in the EDr with the T increase, and the R² for the best-fitted model was R² = 0.41. The EDr of CSF produced from plastic increased as the T increased to 460 °C and then started to decrease. The highest R² for the plastic model was 0.55 (Table 1). The CSF from rubber was characterized by a decrease in the EDr as the T increased, and the R² for the best model was 0.88. The EDr of CSF produced from PAP/AL/PE composite packaging pack increased with T increase up to 460 °C and then started decrease. The R² for the best model was 0.73. The CSF produced from wood was characterized by an increase in the EDr as the T increased, and the R² for the best-fitted model was 0.82 (Table 2).

The EDr results showed that for fabric, kitchen waste, PAP/AL/PE composite packaging pack, and wood, the higher T, the higher energy becomes concentrated in CSF even up to EDr = 1.4. The opposite tendency was for plastic and rubber, for which pyrolysis led to a decrease in EDr < 1. This means that the CSF had less energy than the substrate used for its production. This phenomenon might be due to the higher rate of AC increase than FC rate, thus, lower EDr in these CSFs.

The correlation between the experiment and the model data for EDr is shown in Figure 2. The correlation between the proposed general model and experimental data was 85% for RDF blend 1 and 87% for RDF blend 2, respectively. It means that based on pyrolysis' T, t, and knowledge of RDF composition share, it is possible to predict the energy densification ratio of RDF after its carbonization.

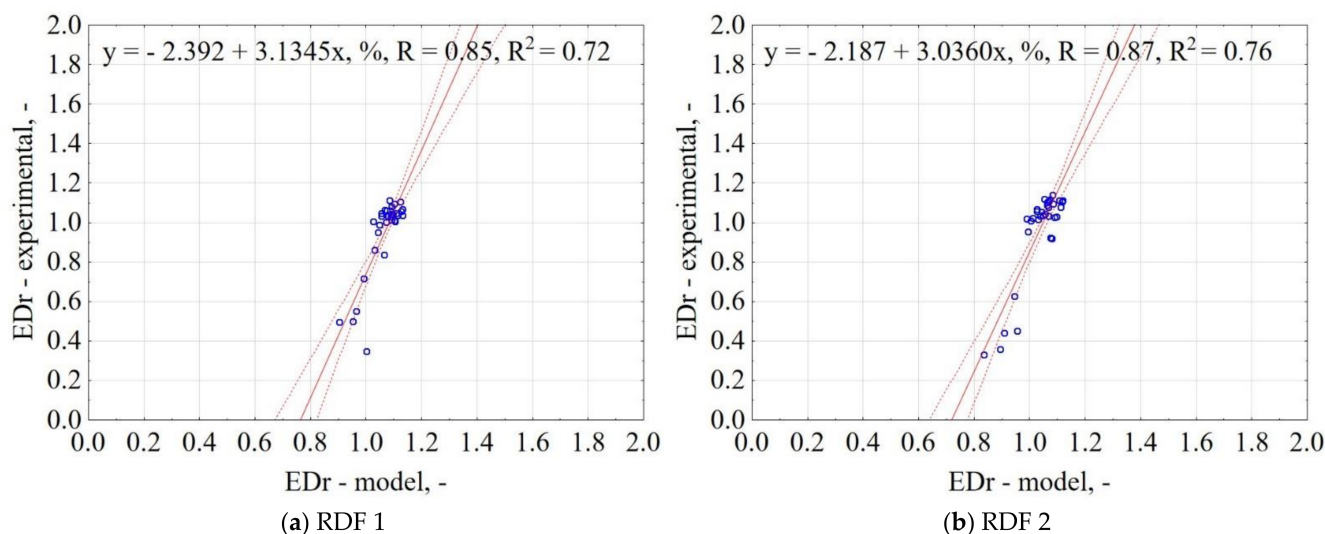


Figure 2. Correlation between experimental and predicted energy densification ratio (EDr) of carbonized RDF blends, (a) RDF 1, (b) RDF 2. Blue circles indicate the experimental and predicted data.

3.1.3. Energy Yield of CSF

For all EY, model IV turned out to be the best-fitted model, except for plastic and rubber, for which model II was better (Table A1). These models' equations presenting the influence of low-temperature pyrolysis T and t on the EY were shown in Table 3.

Table 3. The chosen (best-fitted) mathematical models of the influence of the pyrolysis temperature and residence time on the EY of CSF produced from different RDF components.

Material	Equation	R ²
Carton	$EY(T,t) = 463.255 - 1.50599 \times T - 3.38498 \times t + 0.00135398 \times T^2 + 0.00995947 \times t^2 + 0.00536615 \times T \times t$	0.76
Fabric	$EY(T,t) = 644.004 - 2.29865 \times T - 4.12665 \times t + 0.00222253 \times T^2 + 0.0151381 \times t^2 + 0.00597733 \times T \times t$	0.81
Kitchen waste	$EY(T,t) = 350.058 - 1.14163 \times T - 1.55505 \times t + 0.0011033 \times T^2 + 0.00316085 \times t^2 + 0.00261416 \times T \times t$	0.81
Paper	$EY(T,t) = 473.744 - 1.61526 \times T - 3.26723 \times t + 0.0015321 \times T^2 + 0.0111973 \times t^2 + 0.00497287 \times T \times t$	0.81
Plastic	$EY(T,t) = -9.37476 + 0.90073 \times T - 0.00130925 \times T^2 - 2.83805 \times t + 0.0328112 \times t^2$	0.24
Rubber	$EY(T,t) = 264.858 - 0.388561 \times T - 5.14248 \cdot 10^{-5} \times T^2 - 1.56949 \times t + 0.0114869 \cdot t^2$	0.85
PAP/AL/PE composite packaging pack	$EY(T,t) = -53.6102 + 1.01489 \times T - 0.678159 \times t - 0.00150398 \times T^2 + 0.0150335 \times t^2 - 0.00239616 \times T \times t$	0.78
Wood	$EY(T,t) = 311.037 - 0.913675 \times T - 1.84836 \times t + 0.00080429 \times T^2 + 0.00715877 \times t^2 + 0.00261271 \times T \times t$	0.79

The EY of CSF from carton decreased with increasing T and t from 97% to 35% model R² = 0.76. Pyrolysis of the fabric was characterized by a decrease in EY along with an increase in T and t from 96% to 26%, model R² = 0.81. The CSF from kitchen waste was characterized by decreased EY with an increase in T and t from 93% to 47%, model R² = 0.81. The EY of CSF from paper decreased with increasing T and t from 99.9% to 28%, model R² = 0.81. The CSF from plastic was characterized by a decrease in EY along with an increase in T and t from 98% to 8%, model R² = 0.24. The EY of CSF from rubber decreased with increasing T and t from 99% to 20%, model R² = 0.85. The EY of the CSF made from the PAP/AL/PE composite packaging pack was characterized by a decrease with increasing T from 99% to 25%, model R² = 0.78. Wood pyrolysis was characterized by a decrease in the EY along with an increase in T and t from 98% to 41%, model R² = 0.79.

The results showed that for all MSW/RDF components, the EY decreases with the increase of T and t. The decrease in EY of solid fractions with increasing T is typical for most materials converted thermally [35,36]. Despite increased HHVs, the EY decreased due to the significant decrease in MY of the CSFs [37].

The correlation between the experiment and the model for EY is shown in Figure 3. The confidence interval was 95%. The results showed that the proposed model explains 74% and 61% of data variability for RDF blend 1 and RDF blend 2, respectively. The obtained results indicate that it is possible to predict EY with accuracy over >60% based on pyrolysis T, t, and RDF composition share.

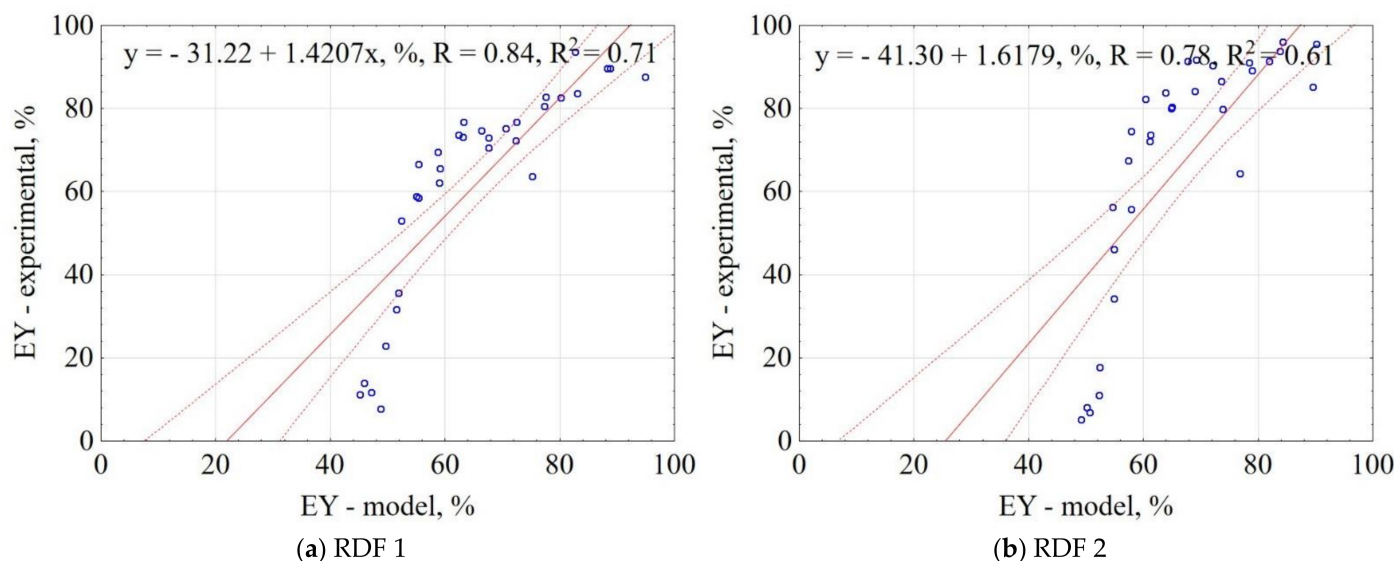


Figure 3. Correlation between experimental and predicted energy yield (EY) of carbonized RDF blends, (a) RDF blend 1, (b) RDF blend 2. Blue circles indicate the experimental and predicted data.

3.1.4. Moisture Content of CSF

For most MC models, model IV was the best fitted, but for fabric and PAP/AL/PE composite packaging pack, model II was better, and for the wood model I (Table A2). The best-fitted equations of influence of T and t on the MC of CSF are presented in Table 4.

Table 4. The chosen (best-fitted) mathematical models of the influence of the pyrolysis T and t on the moisture content (MC) of CSF produced from different RDF components.

Material	Equation	R ²
Carton	$MC(T,t) = 4.45356 - 0.0162423 \times T + 0.0509884 \times t + 2.81284 \cdot 10^{-5} \times T^2 + 0.000382481 \times t^2 - 0.000179923 \times T \times t$	0.11
Fabric	$MC(T,t) = -9.21332 + 0.0470837 \times T - 5.06548 \cdot 10^{-5} \times T^2 + 0.0599597 \times t - 0.000364179 \times t^2$	0.13
Kitchen waste	$MC(T,t) = -3.55952 + 0.0185074 \times T + 0.116747 \times t - 6.46219 \times 10^{-6} \times T^2 - 0.000707797 \times t^2 - 0.000144938 \times T \times t$	0.10
Paper	$MC(T,t) = 21.8367 - 0.0859335 \times T - 0.0675578 \times t + 9.25108 \cdot 10^{-5} \times T^2 - 0.000173046 \times t^2 + 0.000177062 \times T \times t$	0.21
Plastic	$MC(T,t) = 8.3711 - 0.0361188 \times T - 0.0326103 \times t + 4.02833 \times 10^{-5} \times T^2 + 0.00016858 \times t^2 + 5.13878 \times 10^{-5} \times T \times t$	0.35
Rubber	$MC(T,t) = 2.14313 - 0.00478142 \times T - 0.0373156 \times t + 3.77281 \times 10^{-6} \times T^2 + 0.000197849 \times t^2 + 6.01358 \times 10^{-5} \times T \times t$	0.05
PAP/AL/PE composite packaging pack	$MC(T,t) = 29.7302 - 0.135813 \times T + 0.000164348 \times T^2 - 0.053865 \times t + 0.000720295 \times t^2$	0.49
Wood	$MC(T,t) = 0.992658 + 0.00451654 \times T + 0.00649111 \cdot t$	0.05

The MC of CSF from carton ranged from 0.51% to 4.19%, with no linear relationship. The highest MC was observed for CSF produced at 300 °C and 60 min, while the lowest for CSF produced at 20 min and 300–440 °C, model $R^2 = 0.11$. The CSF from cotton had an MC of 0.16% to 7.86%. The highest MC was found in CSF produced at 60 min & 440–500 °C, while the lowest at 20 min at 300–320 °C, model $R^2 = 0.13$. The MC of CSF from kitchen waste ranged from 0.36% to 7.22%. The highest MC was found in CSFs produced at 20–40 min and 440–500 °C, model $R^2 = 0.10$. CSF made from the paper had an MC of 0.34% to 6.23%. The highest MC was observed in CSF produced at 300 °C and the lowest at 360–420 °C, model $R^2 = 0.21$. The results of the MC of CSF made from plastic ranged from 0.01% to 1.36%. The highest MC was in CSF produced at 300 °C, whereas the lowest in CSF produced at 400–460 °C, model $R^2 = 0.35$. CSF made of rubber had an MC of 0.1% to 2.37%. The highest MC was found in CSF produced at 440–500 °C in 60 min and the lowest at 480 °C in 40 min, model $R^2 = 0.05$. The MC of CSF from PAP/AL/PE composite packaging pack waste was between 0.18% and 5.21%. The highest MC was observed for CSF produced at the lowest and highest T (at 300 °C and 500 °C), while the lowest MC at 380–420 °C, model $R^2 = 0.49$. The results of MC of CSF from wood ranged from 0.08% to 6.25%. The highest MC was found in CSF produced at 480–500 °C, while the lowest MC was found in CSF produced at 300 °C, model $R^2 = 0.05$.

The proposed model of MC for CSF had R^2 ranging from 0.05–0.49. The reason for that could be that CSF samples were generated and stored for a long time before MC determination. Similar results (no tendency) were found in our previous work about torrefaction [16]. For that reason, additional tests should be done to reveal the cause of that phenomenon.

The correlation between the experiment and the model data for MC is shown in Figure 4. The results showed that the proposed model could not predict the MC of CSF, and it explains only 2% and 10% of data variability for RDF blend 1 and RDF blend 2, respectively. The MC of CSF was characterized by high scatter. Caution should be exercised with the proposed model for MC.

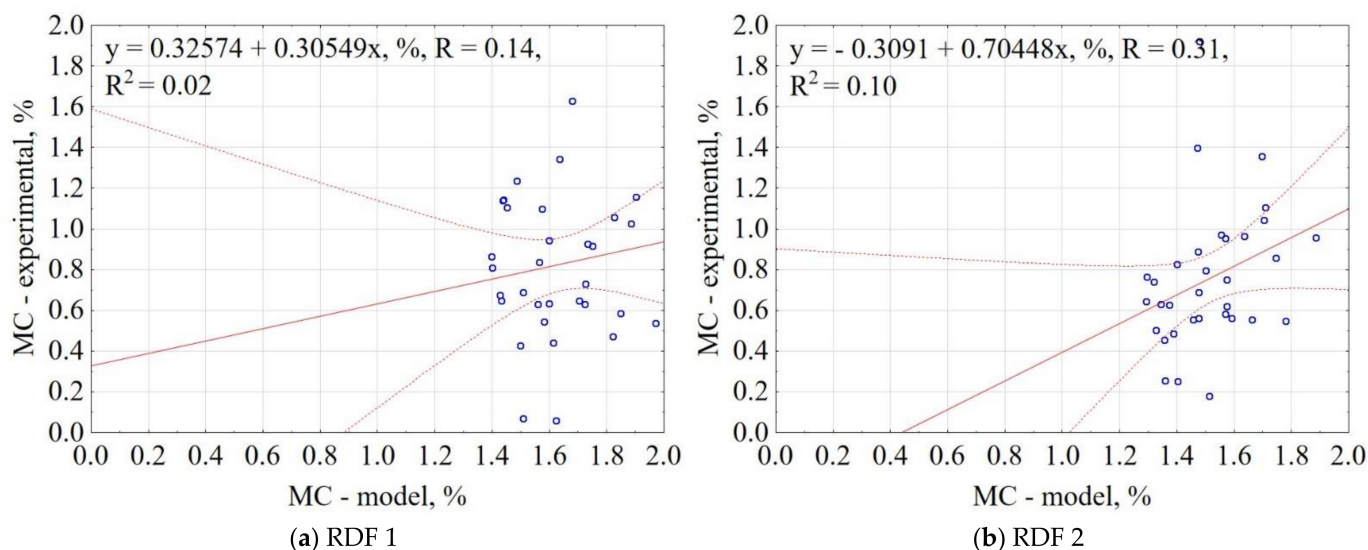


Figure 4. Correlation between experimental and predicted moisture content (MC) of carbonized RDF blends, (a) RDF blend 1, (b) RDF blend 2. Blue circles indicate the experimental and predicted data.

3.1.5. Organic Matter Content of CSF

For most OM models, model IV was the best fitted, except fabric and wood, for which the best model was model II (Table A2). The equations of influence of low-temperature pyrolysis T and t on the OM of CSF are shown in Table 5.

Table 5. The chosen mathematical models of the influence of the pyrolysis temperature and residence time on the organic matter content (OM) content of CSF produced from different RDF components are given.

Material	Equation	R ²
Carton	$OM(T,t) = 211.614 - 0.475308 \times T - 1.51295 \times t + 0.000401745 \times T^2 + 0.0108101 \times t^2 + 0.00120767 \times T \times t$	0.78
Fabric	$OM(T,t) = 99.7307 + 0.00951611 \times T - 2.04132 \times 10^{-5} \times T^2 - 0.0610921 \times t + 0.000676729 \times t^2$	0.31
Kitchen waste	$OM(T,t) = 114.173 - 0.0560588 \times T - 0.923412 \times t - 9.10507 \times 10^{-5} \times T^2 + 0.00277531 \times t^2 + 0.00161421 \times T \times t$	0.49
Paper	$OM(T,t) = 228.645 - 0.608106 \times T - 1.07174 \times t + 0.000466622 \times T^2 - 0.000843949 \times t^2 + 0.00244208 \times T \times t$	0.72
Plastic	$OM(T,t) = -370.952 + 2.24812 \times T + 2.39959 \times t - 0.00265716 \times T^2 + 0.00200287 \times t^2 - 0.00736942 \times T \times t$	0.69
Rubber	$OM(T,t) = 54.0888 + 0.236418 \times T + 0.269375 \times t - 0.000443141 \times T^2 - 0.00150753 \times t^2 - 0.00107728 \times T \times t$	0.84
PAP/AL/PE composite packaging pack	$OM(T,t) = -9.35866 + 0.604654 \times T - 0.329619 \times t - 0.000867447 \times T^2 + 0.00510722 \times t^2 - 0.000765698 \times T \times t$	0.83
Wood	$OM(T,t) = 104.571 - 0.00912015 \times T - 1.92896 \times 10^{-5} \times T^2 - 0.321397 \times t + 0.00329522 \times t^2$	0.49

The OM in CSF from carton ranged from 44% to 83%. As the T and t increased, OM's content in CSF decreased, model R² = 0.78. CSF produced from the fabric contained ~99.5% of OM. The increase of T and t slightly led to a decrease in OM, model R² = 0.28–0.31. The OM in CSF produced from kitchen waste ranged from 50% to 83%, model R² = 0.49. The results of the OM of CSF produced from paper ranged from 29% to 78%. As the T and t increase, the OM in CSF decreased, model R² = 0.72. CSF made from plastic contained OM in the range from 4% to 87%, model R² = 0.69. The content of OM in CSF made of rubber ranged from 47% to 86%. As the T and t increase, the OM in CSF decreased, model R² = 0.84. CSF produced from PAP/AL/PE composite packaging pack waste had OM between 49% and 87%. As the T and t increase, the OM in CSF decreased, model R² = 0.83. The OM in CSF made from wood ranged from 83% to 98%. In general, the increase in T led to a decrease in OM, model R² = 0.49.

The proposed models of OM in CSF made from MSW components had low (e.g., fabric, wood) and high R² (eq. carton, rubber), respectively. Despite the low R² for fabric and wood, the models should reflect the general trend in the experimental data because the OM showed a decreasing linear relationship with an increase in T, and the differences in OM for CSF produced at 300 and 500 °C were low. The general trend in the decrease of OM in CSF with an increase of T and t was observed. This finding is in agreement with previous work [12]. The OM decrease is a result of OM volatilization. During pyrolysis, the processed material molecules are thermally decomposed (breaking into smaller ones), vaporized, and off-gased. The volatilization is also dependent on the pyrolysis T, and it increases when T increase.

The correlation between the experiment and the model data for OM is shown in Figure 5. The results showed that the proposed model explains 77% of the data variability for RDF 1 and RDF 2, respectively. The confidence interval was 95%. The largest concentration of results is in the range 80–85% for experimental data and 75–85% for models, which means the model lowers the value slightly. The results indicate that based on the assumptions of pyrolysis T, t, RDF components share, it is possible to predict the OM in carbonized RDF.

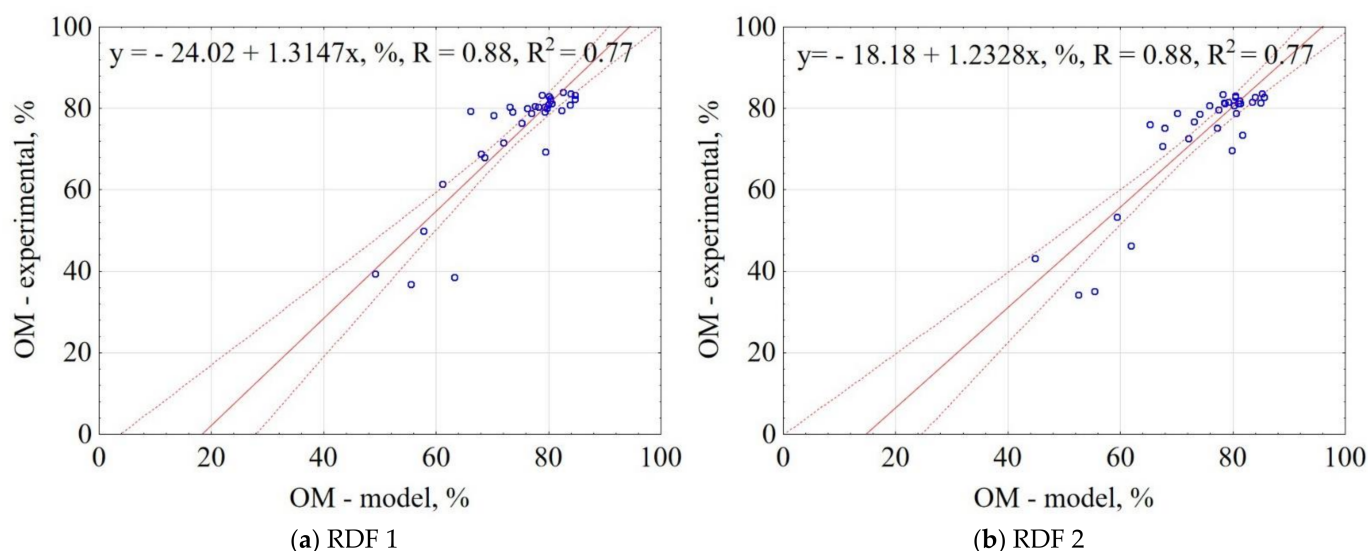


Figure 5. Correlation between experimental and predicted organic matter content (OM) of carbonized RDF blends, (a) RDF blend 1, (b) RDF blend 2. Blue circles indicate the experimental and predicted data.

3.1.6. Ash Content of CSF

For most AC models, model IV turned the best fitted. The best-fitted models for fabric and wood were I and II, respectively (Table A2). These equations are shown in Table 6.

Table 6. The chosen (best-fitting) mathematical models of the influence of the pyrolysis temperature and residence time on the AC of CSF produced from different RDF components.

Material	Equation	R ²
Carton	$AC(T,t) = -95.544 + 0.392259 \times T + 1.24361 \times t - 0.000333039 \times T^2 - 0.00830639 \times t^2 - 0.0010555 \times T \times t$	0.84
Fabric	$AC(T,t) = 0.127194 - 0.00312043 \times T + 8.32241 \times 10^{-6} \times T^2 + 0.012343 \times t - 7.1599 \times 10^{-5} \times t^2$	0.35
Kitchen waste	$AC(T,t) = -10.3584 + 0.0434269 \times T + 0.612167 \times t + 2.97628 \times 10^{-5} \times T^2 - 0.00231362 \times t^2 - 0.000874366 \times T \times t$	0.40
Paper	$AC(T,t) = -93.6731 + 0.428111 \times T + 0.630943 \times t - 0.000347455 \times T^2 + 0.000742667 \times t^2 - 0.00141276 \times T \times t$	0.63
Plastic	$AC(T,t) = 285.315 - 1.33859 \times T - 1.72824 \times t + 0.00156606 \times T^2 + 0.00119026 \times t^2 + 0.00477206 \times T \times t$	0.77
Rubber	$AC(T,t) = 31.3507 - 0.160593 \times T - 0.224709 \times t + 0.000313069 \times T^2 + 0.00295488 \times t^2 + 0.000553607 \times T \times t$	0.78
PAP/AL/PE composite packaging pack	$AC(T,t) = 68.7329 - 0.416816 \times T + 0.333945 \times t + 0.000643374 \times T^2 - 0.00512668 \times t^2 + 0.000646058 \times T \times t$	0.86
Wood	$AC(T,t) = -0.0557718 + 0.000621897 \times T + 1.61345 \times 10^{-5} \times T^2 + 0.120489 \times t - 0.00101243 \times t^2$	0.32

The AC of CSF made from cartons ranged from 10% to 40%. As the T and t increased, the AC increased, model R² = 0.84. The CSF produced from the fabric had an AC of ~1%, model R² = 0.35. The AC of CSF produced from kitchen waste ranged from 8% to 29%, model R² = 0.40. The CSF made from paper contained AC between 3% and 41%, model R² = 0.63. AC in CSF made of plastic was between 8% and 58%, model R² = 0.77. The CSF made of rubber contained AC between 11% and 47%, model R² = 0.78. The AC of CSF made from PAP/AL/PE composite packaging pack ranged from 7% to 45%, model R² = 0.86. The CSF made from wood had an AC ranging from 0.7% to 12%, model R² = 0.32.

For each material, as the T and t increased, the AC increased. The observed trend is typical for CSF, the OM is removed from the processed material in gases and tar while the inorganic fraction remains [38,39]. The biggest surprise was the increase of AC for CSF

made from plastic at 500 °C at 60 min, where its content increased almost to 60%. The reason for that could be that the reactor was flushed with CO₂ gas, and as a result, no secondary reaction could form a char from liquids [34]. The other explanation for that phenomenon may be the Boudouard reaction (CO₂ + C = 2CO), where char could be transformed into CO. Nevertheless, the Boudouard reaction can occur at higher temperatures >700 °C [40]. The partial oxidation (incineration) of the plastic is rather unlikely because all RDF components were pyrolyzed at the same time, and the other types of samples did not show the same tendency.

The correlation between the experiment and the model data for AC is shown in Figure 6. The results showed that the proposed model explains 66% and 69% of data variability for RDF blend 1 and RDF blend 2, respectively. The confidence interval was 95%. The obtained results indicate that based on the assumptions of pyrolysis T, t, and knowledge of RDF composition, it is possible to predict the AC of carbonized RDF.

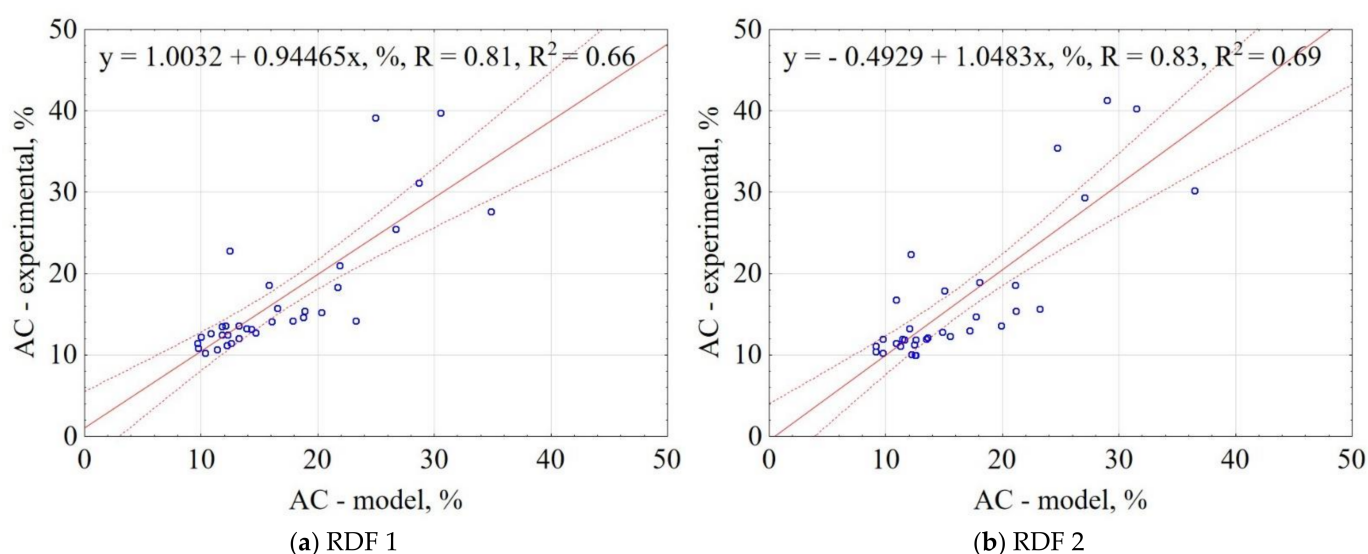


Figure 6. Correlation between experimental and predicted ash content (AC) of carbonized RDF blends, (a) RDF blend 1, (b) RDF blend 2. Blue circles indicate the experimental and predicted data.

3.1.7. Combustible Parts of CSF

For most CP models, model IV was the best fitted, but for fabric and wood better were models I and II, respectively (Table A2). The equations describing the influence of low-temperature pyrolysis T and t on the CP of CSF are summarized in Table 7.

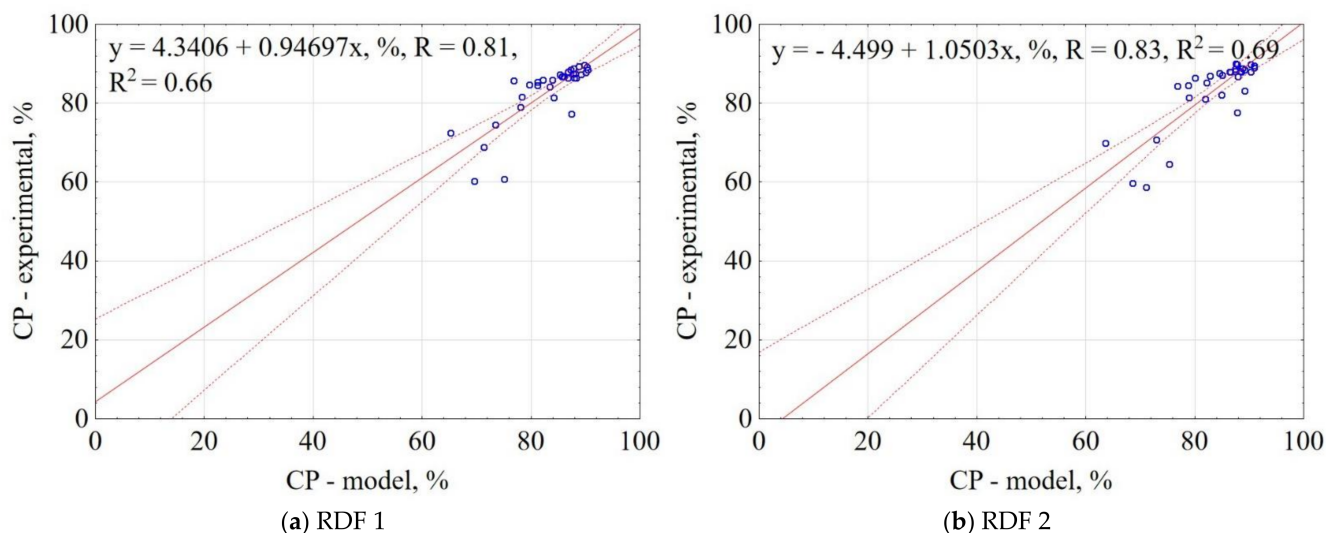
The CP in the CSF formed from the carton ranged from 59% to 90%, model $R^2 = 0.84$. The CSF from the fabric contained 97% to 99% of the CP, model $R^2 = 0.35$. The content of CP in CSF produced from kitchen waste ranged from 71% to 89%, model $R^2 = 0.40$. The CSF made from paper contained 58% to 96% of CP, model $R^2 = 0.63$. The CP in CSF made from plastic ranged from 42% to 91%, model $R^2 = 0.77$. The CSF made of rubber contained 52% to 89% of CP, $R^2 = 0.78$. The content of CP in the CSF made from PAP/AL/PE composite packaging pack ranged from 55% to 93%, model $R^2 = 0.86$. The CSF from wood contained 89% and 99% of CP, model $R^2 = 0.32$.

Table 7. The chosen (best-fitting) mathematical models of the influence of the pyrolysis temperature and residence time on the combustible parts (CP) of CSF produced from different RDF components.

Material	Equation	R ²
Carton	$CP(T,t) = 195.544 - 0.392259 \times T^{-1} \cdot 2.4361 \times t + 0.000333039 \times T^2 + 0.00830639 \times t^2 + 0.0010555 \times T \times t$	0.84
Fabric	$CP(T,t) = 99.8728 + 0.00312028 \times T - 8.32223 \times 10^{-6} \times T^2 - 0.012343 \times t + 7.1599 \cdot 10^{-5} \times t^2$	0.35
Kitchen waste	$CP(T,t) = 110.358 - 0.0434266 \times T - 0.612168 \times t - 2.97632 \times 10^{-5} \times T^2 + 0.00231363 \times t^2 + 0.000874366 \times T \times t$	0.40
Paper	$CP(T,t) = 194.858 - 0.433983 \times T - 0.632625 \times t + 0.000354099 \times T^2 - 0.000849486 \times t^2 + 0.0014323 \times T \times t$	0.63
Plastic	$CP(T,t) = -185.315 + 1.33859 \times T + 1.72824 \times t - 0.00156606 \times T^2 - 0.00119026 \times t^2 - 0.00477206 \times T \times t$	0.77
Rubber	$CP(T,t) = 68.6493 + 0.160593 \times T + 0.224709 \times t - 0.000313069 \times T^2 - 0.00295489 \times t^2 - 0.000553607 \times T \times t$	0.78
PAP/AL/PE composite packaging pack	$CP(T,t) = 31.2671 + 0.416816 \times T - 0.333945 \times t - 0.000643374 \times T^2 + 0.00512668 \times t^2 - 0.000646058 \times T \times t$	0.86
Wood	$CP(T,t) = 100.096 - 0.000577691 \times T^{-1} \times 62655 \cdot 10^{-5} \times T^2 - 0.122004 \times t + 0.00102758 \times t^2$	0.32

The decreasing trend of CP with an increase of T and t is typical and very similar to the OM. A decrease of CP in RDF pyrolyzed was previously reported by Stępień et al. [5]. Carbonized RDF resulted in the CP decrease (from 81% to 43%) and AC increase (from 18% to 57%) [5].

The correlation between the experiment results and the model data for CP is shown in Figure 7. The results showed that the proposed model explained 66% and 69% of data variability for RDF blend 1 and RDF blend 2, respectively. The confidence interval was 95%. The obtained results indicate that based on the assumptions of pyrolysis T, t, and RDF composition, it is possible to predict the CP of carbonized RDF.

**Figure 7.** Correlation between experimental and predicted combustible parts (CP) of carbonized RDF blends, (a) RDF blend 1, (b) RDF blend 2. Blue circles indicate the experimental and predicted data.

3.1.8. Carbon Content of CSF

For all tested materials, the C was described best by model IV (Table A3). The equations of influence of low-temperature pyrolysis T and t on the C of CSF are summarized in Table 8.

Table 8. The chosen (best-fitting) mathematical models of the influence of the pyrolysis temperature and residence time on the C of CSF produced from different RDF components.

Material	Equation	R ²
Carton	$C(T,t) = 14.9394 + 0.110664 \times T + 0.27 \times t - 9.22688 \times 10^{-5} \times T^2 + 0.001 \times t^2 - 0.000734091 \times T \times t$	0.46
Fabric	$C(T,t) = -139 + 0.776403 \times T + 1.32727 \times t - 0.000759518 \times T^2 - 0.00727273 \times t^2 - 0.00154545 \times T \times t$	0.62
Kitchen waste	$C(T,t) = 111.158 - 0.329169 \times T + 0.342273 \times t + 0.00041453 \times T^2 - 0.00179546 \times t^2 - 0.000393182 \times T \times t$	0.26
Paper	$C(T,t) = 43.697 - 0.0542969 \times T + 0.429545 \times t + 0.00010878 \times T^2 - 0.000568175 \times t^2 - 0.000886363 \times T \times t$	0.24
Plastic	$C(T,t) = -207.545 + 1.34185 \times T + 2.12727 \times t - 0.0015472 \times T^2 + 9.26989 \times 10^{-10} \times t^2 - 0.00609091 \times T \times t$	0.72
Rubber	$C(T,t) = 118.755 - 0.131543 \times T + 0.118908 \times t + 6.15577 \times 10^{-5} \times T^2 - 0.00221363 \times t^2 - 0.000437044 \times T \times t$	0.69
PAP/AL/PE composite packaging pack	$C(T,t) = -144.424 + 0.858967 \times T + 1.63864 \times t - 0.000925602 \times T^2 - 0.00511364 \times t^2 - 0.00310227 \times T \times t$	0.63
Wood	$C(T,t) = 43.6364 - 0.0147981 \times T + 0.523864 \times t + 0.000107323 \times T^2 - 0.00073864 \times t^2 - 0.000903409 \times T \times t$	0.72

In general, for CSF from fabric and wood, the increase of T and t increased the C. An opposite trend was observed for plastic and rubber where CSF produced at lower T had higher C. No impact of T and t on the C of CSF made from the carton, paper, and kitchen waste was observed. The C of CSF made from the carton ranged from 39% to 48%, and the highest R² was 0.46. The C of CSF made from fabric ranged from 43% to 73%, and the highest R² was 0.62. The CSF produced from kitchen waste contained 41% to 59% of C, and the highest R² was 0.26. The C of CSF made from paper ranged from 35% to 46%, and the highest R² was 0.24. The CSF made from plastic contained between 13% and 73% of C, and the highest R² was 0.72. The C of CSF made from rubber was in the range of 55% to 85%, and for the best-fitted model, R² = 0.69. The CSF from the PAP/AL/PE composite packaging pack contained between 35% and 62% of C and the best-fitted model had R² = 0.63. The C of CSF made from wood was between 47% and 67%, and the best-fitted model had R² = 0.72.

The trends of C changes on studied materials are in agreement with previous research. In general, decarbonization of the substrate occurs during pyrolysis, and an increase of C content in char compared to the untreated substrate is a result of reduced char mass—the remaining char becomes an increasingly condensed carbon matrix [41]. Muley et al. [41] pyrolyzed cellulose and sawdust at temperatures from 500 °C to 700 °C and found that the C increased from 42% to 79% and 47% to 89%, respectively. In the present study, cellulose materials (carton, fabric, paper) pyrolyzed at 500 °C had C in the range of 44–60% and did not show such a large increase, probably because of too low pyrolysis T. Quite interesting is the observed decrease in C in rubber from 80% to 56%. In the work of Mui et al. [42], waste tire rubber was carbonized at 400–900 °C and showed the opposite trend, where the C increased from 80% to 88% [42]. On the other hand, Acosta et al. [43] showed that scrap tires' carbonization at 570 °C led to a decrease in C from 86% to 80%. These differences may be a result of the different compositions of carbonized rubber.

The correlation between the experiment and the model data for C is shown in Figure 8. The results showed that the proposed model explained 76% and 74% of data variability for RDF blend 1 and RDF blend 2, respectively. The confidence interval was 95%. The largest concentration of results was 60–65% of C for the experimental and the modeled data. The obtained results indicate that based on pyrolysis T, t, and knowledge of RDF composition, it is possible to predict the C in CSF.

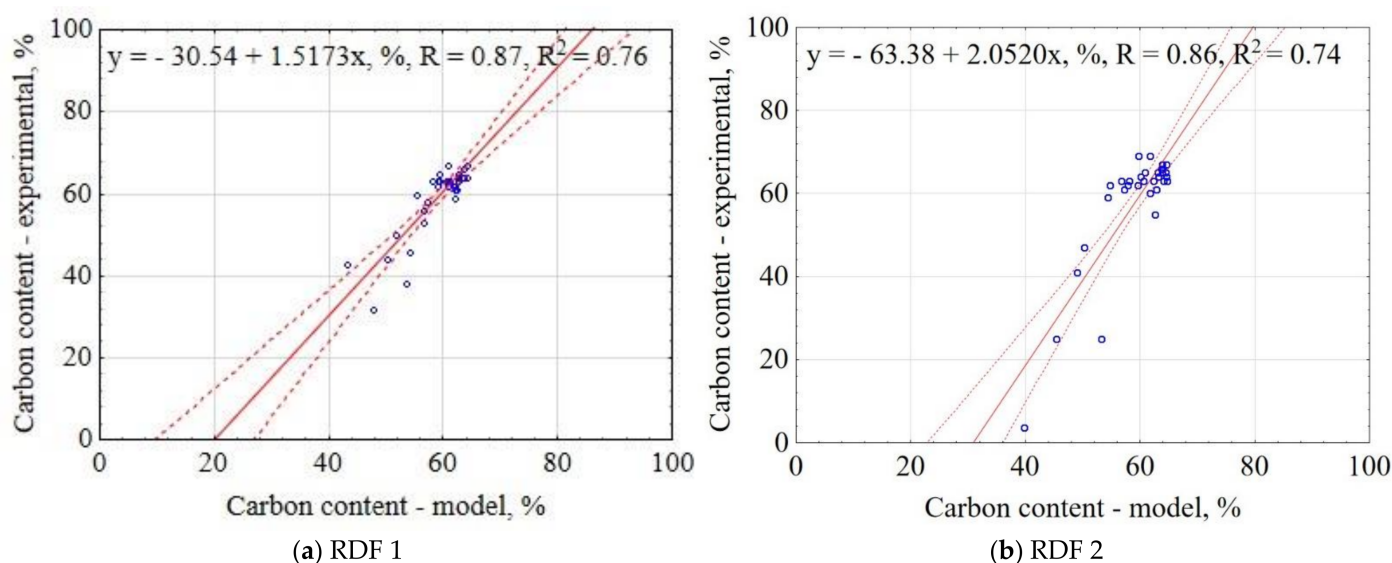


Figure 8. Correlation between experimental and predicted carbon content (C) of carbonized RDF blends, (a) RDF blend 1, (b) RDF blend 2. Blue circles indicate the experimental and predicted data.

3.1.9. Hydrogen Content of CSF

For H determination in CSF, the best model type was model IV, except for kitchen waste, where model II had the better fit (Table A3). The equations of influence of low-temperature pyrolysis T and t on the H of CSF are summarized in Table 9.

Table 9. The chosen (best-fitting) mathematical models of the influence of the pyrolysis temperature and residence time on the H content of CSF produced from different RDF components.

Material	Equation	R ²
Carton	$H(T,t) = 25.7364 - 0.0817727 \times T - 0.156818 \times t + 7.95455 \times 10^{-5} \times T^2 + 0.00120455 \times t^2 + 8.63636 \times 10^{-5} \times T \times t$	0.92
Fabric	$H(T,t) = 34.3758 - 0.114567 \times T - 0.164091 \times t + 0.000107906 \times T^2 + 6.81809 \times 10^{-5} \times t^2 + 0.000285227 \times T \times t$	0.79
Kitchen waste	$H(T,t) = 15.6939 - 0.041657 \times T + 3.73932 \times 10^{-5} \times T^2 - 0.0625 \times t + 0.000534091 \times t^2$	0.83
Paper	$H(T,t) = 23.429 - 0.0742717 \times T - 0.145876 \times t + 6.72703 \times 10^{-5} \times T^2 + 0.000605284 \times t^2 + 0.000175301 \times T \times t$	0.88
Plastic	$H(T,t) = -44.8006 + 0.276956 \times T + 0.432934 \times t - 0.000314235 \times T^2 + 0.00050216 \times t^2 - 0.00135652 \times T \times t$	0.66
Rubber	$H(T,t) = 26.1644 - 0.0922177 \times T - 0.177385 \times t + 9.00828 \times 10^{-5} \times T^2 + 0.00123522 \times t^2 + 0.000127838 \times T \times t$	0.91
PAP/AL/PE composite packaging pack	$H(T,t) = -20.7405 + 0.15232 \times T + 0.0595576 \times t - 0.000193613 \times T^2 + 0.000570871 \times t^2 - 0.000377273 \times T \times t$	0.72
Wood	$H(T,t) = 4.36363 - 0.00147975 \times T + 0.0523864 \times t + 1.07323 \times 10^{-5} \times T^2 - 7.38636 \times 10^{-5} \times t^2 - 9.03409 \times 10^{-5} \times T \times t$	0.72

For all pyrolyzed materials, as process T and t increased, the H decrease was observed. The exception was wood, for which the H slightly increased. The H of CSF made of carton ranged from 2.1% to 6.3%, and its content decreased when the process T and t increased. The model's R² was 0.92. The CSF made from fabric contained from 2.4% to 7.7% of H, and its content decreased when process T and t increased. The model's R² was 0.79. The CSF produced from kitchen waste contained from 2.1% to 6.2% of H, and its content decreased when process T and t increased. The model's R² was 0.83. The H content of CSF made from the paper was between 1.6% and 5.2%, and its content decreased when process T and t increased. The model's R² was 0.88. CSF made from plastic contained from 3% to 12% H. The H content decreased with an increase in process T. The model R² = 0.66. The H

content of CSF made from rubber contained 0.05% to 3.45% of H, which decreased with an increase in process T. The model R^2 was 0.66. The CSF produced from PAP/AL/PE waste composite packaging pack contained 1.5% to 7.9% of H, which decreased with an increase in T. The model R^2 was 0.72. The H of CSF made of wood ranged from 2.8% to 5.7%, which increased with an increase in process T. The model R^2 was 0.72.

In general, for all pyrolyzed materials, as the T and t increased, the H decreased. The exception to this observation was wood, for which the H increased, which is opposite to the results of Muley et al. [41], Zeng et al. [44], and Ho Kim et al. [45], where H decreases were observed. Nevertheless, similarly to C, the H also is removed during pyrolysis (dehydrogenation) [46] and its content in char compared to the substrate (increase or decrease) depends on the mass reduction of all components.

The correlation between the experiment and the model data for H content is shown in Figure 9. The results showed that the proposed model explained 69% and 74% of data variability for RDF blend 1 and RDF blend 2, respectively. The confidence interval was 95%. The largest concentration of results is in the range of 8–10% for experimental data and 13–15% for the models, which means that the general model slightly overestimates the H in CSF. The obtained results indicate that based on the assumptions of pyrolysis T, t, and RDF composition, it is possible to predict the H in carbonized RDF.

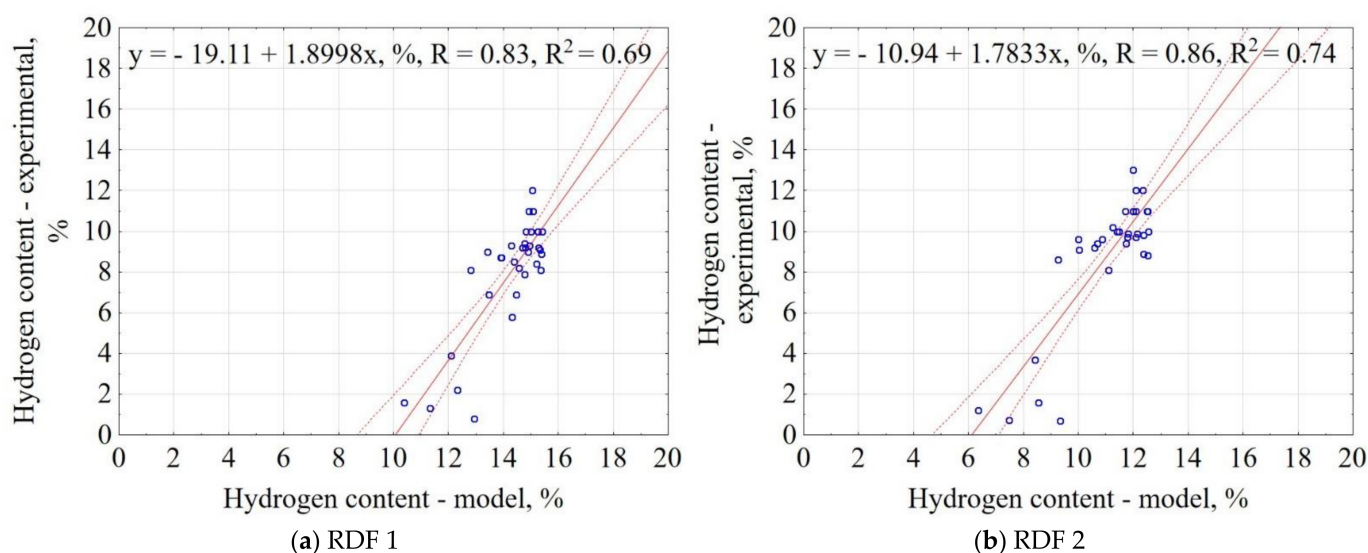


Figure 9. Correlation between experimental and predicted hydrogen content (H) of carbonized RDF blends, (a) RDF blend 1, (b) RDF blend 2. Blue circles indicate the experimental and predicted data.

3.1.10. Nitrogen Content of CSF

For all CSF, the best model for N determination turned out to be model IV. These models IV had the highest R^2 and the lowest AIC value (Table A3). The equations of influence of low-temperature pyrolysis T and t on the N of CSF are summarized in Table 10.

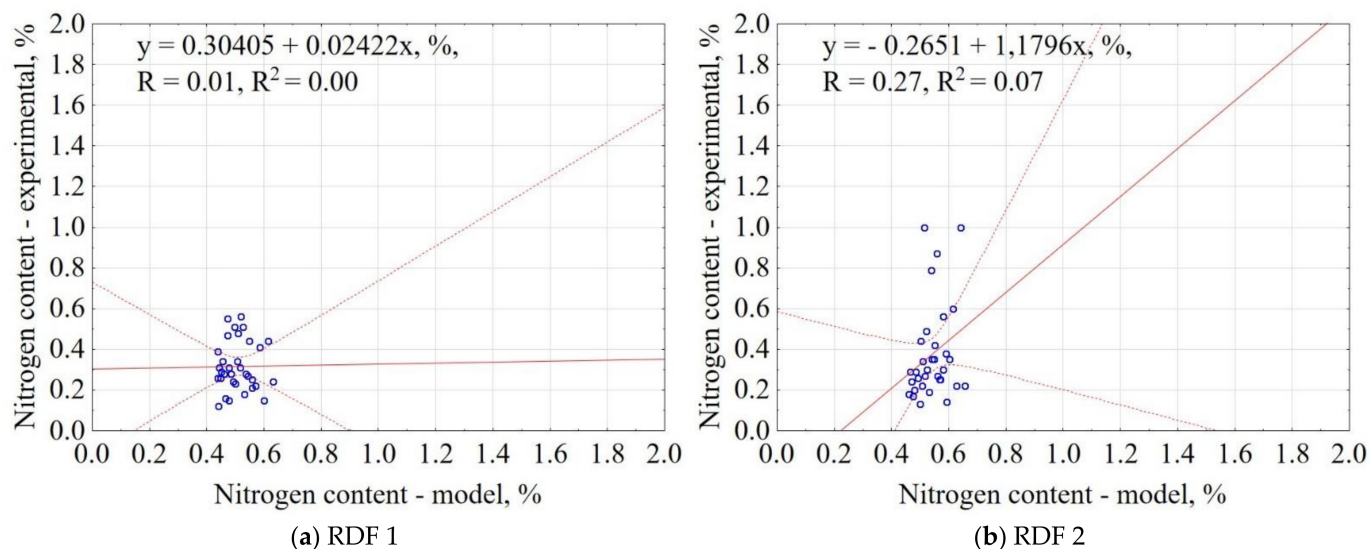
The N of CSF made of carton ranged from 0.1% to 1.7%, and the model had $R^2 = 0.41$. The CSF made from fabric contained from 0.07% to 2% of N, and the model had $R^2 = 0.51$. The CSF produced from kitchen waste contained 2.5% to 7% of N, and the model had $R^2 = 0.46$. For CSF made from the paper, the N was between 0.02% and 0.93%, and the model had $R^2 = 0.69$. The CSF made from plastic contains 0.06% to 7.2% of N, and the model had $R^2 = 0.13$. The N of CSF made of rubber was between 0.12% and 1.72%, and the model $R^2 = 0.38$. The CSF made from PAP/AL/PE composite packaging pack contained from 0.01% to 5.1% of N, and the model $R^2 = 0.21$. The N in CSF from wood ranged from 0.96% to 3.8%, and model $R^2 = 0.46$.

Table 10. The chosen (best-fitting) mathematical models of the influence of the pyrolysis temperature and residence time on the N content of CSF produced from different RDF components.

Material	Equation	R ²
Carton	$N(T,t) = 0.353788 - 0.00163594 \times T + 0.0102094 \times t + 2.79794 \times 10^{-6} \times T^2 - 4.875 \times 10^{-5} \times t^2 - 1.24001 \times 10^{-5} \times T \times t$	0.41
Fabric	$N(T,t) = -0.538518 - 0.00249781 \times T + 0.0363215 \times t + 1.09306 \times 10^{-5} \times T^2 - 0.000272625 \times t^2 - 3.04533 \times 10^{-5} \times T \times t$	0.51
Kitchen waste	$N(T,t) = 7.29638 - 0.0187967 \times T + 0.0120734 \times t + 2.08782 \times 10^{-5} \times T^2 + 8.75 \times 10^{-5} \times t^2 - 4.88262 \times 10^{-5} \times T \times t$	0.46
Paper	$N(T,t) = 0.56423 - 0.00232121 \times T + 0.000358041 \times t + 2.63612 \times 10^{-6} \times T^2 + 8.12501 \times 10^{-6} \times t^2 - 1.61463 \times 10^{-6} \times T \times t$	0.69
Plastic	$N(T,t) = -1.5433 + 0.00661536 \times T + 0.035132 \times t - 8.45851 \times 10^{-6} \times T^2 - 0.000255625 \times t^2 - 2.67845 \times 10^{-5} \times T \times t$	0.13
Rubber	$N(T,t) = 0.183955 - 0.000655605 \times T + 0.0100913 \times t + 1.64191 \times 10^{-6} \times T^2 - 3.25 \times 10^{-5} \times t^2 - 1.45105 \times 10^{-5} \times T \times t$	0.38
PAP/AL/PE composite packaging pack	$N(T,t) = 0.277347 - 0.00120315 \times T + 0.00538399 \times t + 1.20488 \times 10^{-6} \times T^2 - 5.275 \times 10^{-5} \times t^2 - 2.4975 \times 10^{-6} \times T \times t$	0.21
Wood	$N(T,t) = -0.743849 + 0.00728439 \times T + 0.0366098 \times t - 7.02211 \times 10^{-6} \times T^2 + -6.75002 \times 10^{-5} \times t^2 - 6.24626 \times 10^{-5} \times T \times t$	0.46

In general, all N models had low R²; therefore, the proposed models are not suitable for accurate prediction of N content in CSFs, but instead, they can be used to estimate the concentration range for N after pyrolysis.

The correlation between the experiment and the model data is shown in Figure 10. The results showed that the proposed model explained 0% and 7% of data variability for RDF blend 1 and RDF blend 2, respectively. The confidence interval was 95%. The results are characterized by high scatter, which makes the prediction rather not reliable. Based on the proposed model, only the general range of N is possible to check (for tested RDF N content in a narrow range of ~0.4–0.6%)

**Figure 10.** Correlation between experimental and estimated nitrogen content (N) of carbonized RDF blends, (a) RDF blend 1, (b) RDF blend 2. Blue circles indicate the experimental and predicted data.

3.1.11. Sulfur Content of CSF

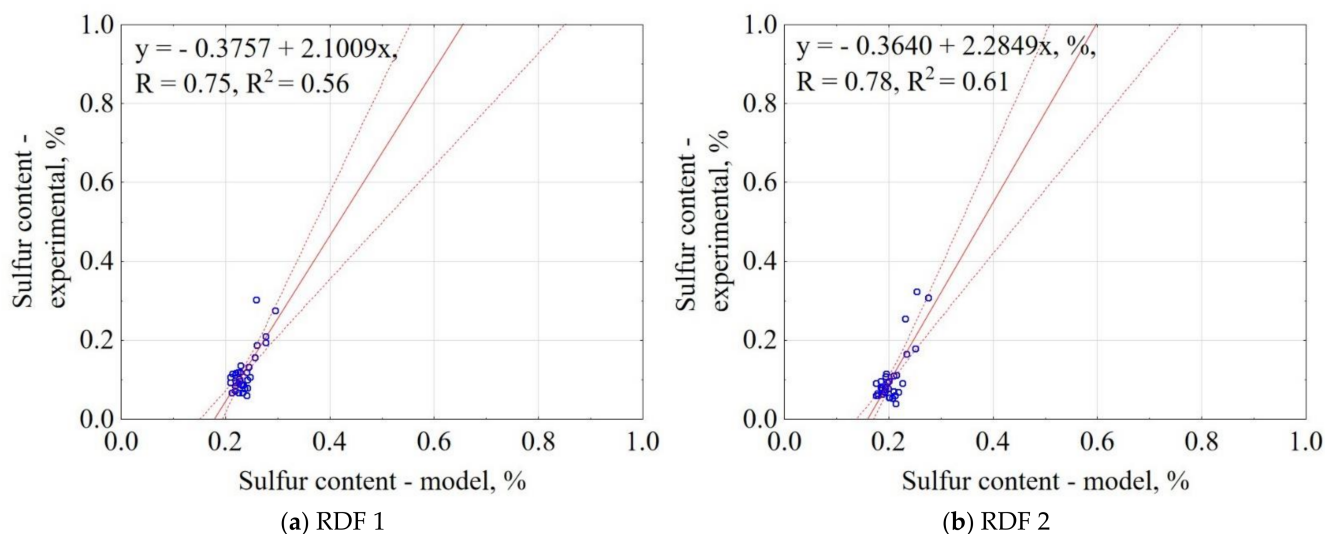
For all CSF, the best model for S determination was model IV. These models IV had the highest R² and the lowest AIC value (Table A3). The equations of influence of low-temperature pyrolysis T and t on the S of CSF are summarized in Table 11.

Table 11. The chosen (best-fitting) mathematical models of the influence of the pyrolysis temperature and residence time on the S content of CSF produced from different RDF components.

Material	Equation	R ²
Carton	$S(T,t) = -0.177334 + 0.000937873 \times T + 0.00420794 \times t - 4.95826 \times 10^{-7} \times T^2 - 8.52128 \times 10^{-7} \times t^2 - 8.69886 \times 10^{-6} \times T \times t$	0.26
Fabric	$S(T,t) = 1.24721 - 0.00598883 \times T + 0.00300454 \times t + 7.38831 \cdot 10^{-6} \times T^2 - 1.59088 \times 10^{-6} \times t^2 - 7.19318 \times 10^{-6} \times T \times t$	0.39
Kitchen waste	$S(T,t) = 0.76394 - 0.00268124 \times T - 0.000843186 \times t + 3.00117 \times 10^{-6} \times T^2 - 4.43179 \times 10^{-6} \times t^2 + 3.75 \times 10^{-6} \times T \times t$	0.35
Paper	$S(T,t) = 0.852576 - 0.00438192 \times T + 0.00400454 \times t + 5.96737 \times 10^{-6} \times T^2 + 9.09103 \times 10^{-7} \times t^2 - 8.71591 \times 10^{-6} \times T \times t$	0.49
Plastic	$S(T,t) = 1.04115 - 0.00503069 \times T - 0.00623409 \times t + 5.96639 \times 10^{-6} \times T^2 + 5.68193 \times 10^{-7} \times t^2 + 1.75341 \times 10^{-5} \times T \times t$	0.78
Rubber	$S(T,t) = 1.3005 + 0.00161075 \times T + 0.00576999 \times t - 1.16336 \times 10^{-6} \times T^2 - 6.05901 \times 10^{-6} \times t^2 - 1.13023 \times 10^{-5} \times T \times t$	0.28
PAP/AL/PE composite packaging pack	$S(T,t) = 0.672402 - 0.00299589 \times T - 0.00228128 \times t + 3.56719 \times 10^{-6} \times T^2 - 1.87036 \times 10^{-6} \times t^2 + 6.33409 \times 10^{-6} \times T \times t$	0.61
Wood	$S(T,t) = 0.278057 - 0.00127582 \times T + 0.00100456 \times t + 1.59488 \times 10^{-6} \times T^2 - 6.11576 \times 10^{-6} \times t^2 - 1.04858 \times 10^{-6} \times T \times t$	0.33

The S in CSF from the carton ranged from 0.01% to 0.21%, and the model had R² = 0.41. The CSF made from cotton contained 0.02% to 0.27% of S, and the model had R² = 0.51. The CSF produced from kitchen waste contained from 0.17% to 0.27% of S, and the model had R² = 0.46. The S of CSF made from the paper was between 0.06% and 0.2%, and the model had R² = 0.69. The CSF made from plastic ranged from 0.01% to 0.18% of S, and the model had low R² = 0.13. S content in CSF made of rubber was from 1.66% to 2.30%, and the model had R² = 0.38. CSF made from PAP/AL/PE composite packaging pack contained from 0.04% to 0.52% of S, and the model had R² = 0.21. The S of CSF produced from wood ranged from 0.03% to 0.40%, and the model had R² = 0.46. These results show that the pyrolysis of MSW components does not cause a significant change in its S content.

The correlation between the experiment and the model for S content is shown in Figure 11. The results showed that the proposed model explained 56% and 61% of data variability for RDF blend 1 and RDF blend 2. The confidence interval was 95%. The largest concentration of results is in 0.1% for experimental data and 0.2% for the models, which means the model overestimated experimental results by approximately a factor of 2.

**Figure 11.** Correlation between experimental and predicted sulfur content (S) of carbonized RDF blends, (a) RDF blend 1, (b) RDF blend 2. Blue circles indicate the experimental and predicted data.

4. Conclusions

The results show that most of the proposed general models had an $R^2 > 0.6$ with experimental data. The best prediction was found for MY ($R^2 = 0.9$). The presented model and the Supplementary Materials spreadsheet with implemented equations are a simple tool to rapidly predict CSF's expected properties made from a specific mixture of common feedstock materials found in MSW. The proposed tool can be used to find the range of pyrolysis T and residence t based on locally available MSW blends, make decisions about an optimized mix of RDF components to obtain the desired CSF quality, depending on its purpose. However, the presented results are based on experimental data from a lab-scale experiment. Therefore, they are not suitable for reuse on an industrial-scale without prior improvement/recalculations related to different plants and units' characteristic technical parameters. Developed models predict what can be expected after carbonization at given process parameters. Nevertheless, each device has its operational parameters that impact the pyrolysis process (heating rate, cooling time, set-up temperature, residence time, feedstock size, etc.). Thus, the models need to be up-scaled and adjusted to the plan/unit-specific available equipment to obtain desired precision.

Supplementary Materials: The following are available online at <https://www.mdpi.com/1996-1944/14/5/1191/s1>, Excel File.

Author Contributions: Conceptualization, K.Ś. and E.S.; methodology, E.S., K.Ś. and P.S.; software, P.S. and K.Ś.; validation, K.Ś. and E.S.; formal analysis, E.S. and K.Ś.; investigation, K.Ś. and E.S.; resources, P.S.; data curation, K.Ś.; writing—original draft preparation, K.Ś. and E.S.; writing—review and editing, E.S., K.Ś., A.B. and J.A.K.; visualization, K.Ś. and E.S.; supervision, A.B. and J.A.K.; project administration, P.S.; funding acquisition, P.S. All authors have read and agreed to the published version of the manuscript.

Funding: The research was supported by the Preludium 14 Program, the National Science Centre, Poland, grant UMO-2017/27/N/ST8/03103 titled “Energy balance of low temperature pyrolysis of organic waste”. Jacek Koziel's participation was partially supported by the Iowa Agriculture and Home Economics Experiment Station, Ames, Iowa. Project no. IOW05556 (Future Challenges in Animal Production Systems: Seeking Solutions through Focused Facilitation) sponsored by Hatch Act & State of Iowa funds. The publication is financed under the Leading Research Groups support project from the subsidy increased for the period 2020–2025 in the amount of 2% of the subsidy referred to Art. 387 (3) of the Law of 20 July 2018 on Higher Education and Science, obtained in 2019.

Institutional Review Board Statement: Not applicable.

Informed Consent Statement: Not applicable.

Data Availability Statement: The data used in this study come from work Świechowski, K.; Syguła, E.; Koziel, J.A.; Stepień, P.; Kugler, S.; Manczarski, P.; Białowiec, A. Low-Temperature Pyrolysis of Municipal Solid Waste Components and Refuse-Derived Fuel—Process Efficiency and Fuel Properties of Carbonized Solid Fuel. *Data* 2020, 5, 48. <https://doi.org/10.3390/data5020048> (accessed on 25 February 2021) and are available in <https://www.mdpi.com/2306-5729/5/2/48/s1> (accessed on 25 February 2021) and data generated in this study are available in the Supplementary materials named “Supplementary Materials-Models”.

Conflicts of Interest: The authors declare no conflict of interest and declare that the funders had no role in the design of the study; in the collection, analyses, or interpretation of data; in the writing of the manuscript, or in the decision to publish the results.

Abbreviations

OECD—Organization for Economic Co-operation and Development

GDP—gross domestic product

MSW—municipal solid waste

MBT—mechanical biological treatment plants

RDF—refuse-derived fuel

CSF—carbonized solid fuel

MY—mass yield

EDr—energy densification ratio

EY—energy yield

MC—moisture content

VM—volatile matter content

FC—fixed carbon content

AC—ash content

CP—combustible parts content

VS—volatile solids content

C, H, N, S—elemental composition, carbon, hydrogen, nitrogen, and sulfur, respectively

T—pyrolysis temperature

t—pyrolysis duration

R²—determination coefficient

AIC—Akaike Information Criterion

Appendix A

Table A1. Results of regression models of pyrolysis process; mass yield (MY), energy densification ratio (EDr), and energy yield (EY) of CSF determined from RDF components concerning pyrolysis temperature and residence time.

Material	Assessment Criterion	Models of MY				Models of EDr				Models of EY			
		I	II	III	IV	I	II	III	IV	I	II	III	IV
Carton	R ²	0.63	0.69	0.69	0.77	0.02	0.16	0.02	0.16	0.64	0.68	0.69	0.76
	AIC	269.52	259.99	259.80	242.24	−76.53	−76.14	−74.64	−75.86	271.89	265.23	261.11	247.88
Fabric	R ²	0.64	0.70	0.68	0.78	0.52	0.54	0.53	0.55	0.66	0.73	0.71	0.81
	AIC	299.28	289.46	293.17	278.17	−2.44	−0.07	−1.00	1.34	290.23	276.34	283.67	261.86
Kitchen waste	R ²	0.66	0.72	0.74	0.85	0.52	0.54	0.53	0.55	0.66	0.71	0.73	0.81
	AIC	245.66	235.55	237.73	220.75	0.07	0.06	0.05	0.04	253.88	247.01	251.22	242.35
Paper	R ²	0.63	0.70	0.68	0.79	0.33	0.41	0.33	0.41	0.65	0.73	0.70	0.81
	AIC	257.79	248.73	245.51	226.40	−72.45	−72.63	−70.52	−70.70	271.30	260.61	262.42	243.58
Plastic	R ²	0.47	0.62	0.51	0.72	0.21	0.43	0.30	0.57	0.18	0.24	0.18	0.24
	AIC	312.00	302.08	302.03	283.52	−15.05	−21.19	−16.56	−28.02	320.15	319.00	322.13	320.97
Rubber	R ²	0.84	0.85	0.84	0.85	0.84	0.86	0.86	0.88	0.84	0.85	0.84	0.85
	AIC	256.65	259.79	257.96	261.08	−44.35	−44.54	−46.08	−46.81	273.34	275.75	274.75	277.13
PAP/AL/PE composite packaging pack	R ²	0.81	0.82	0.82	0.83	0.01	0.52	0.21	0.73	0.69	0.77	0.70	0.78
	AIC	253.00	243.88	253.84	252.39	8.40	−11.52	2.63	−28.25	281.43	274.41	281.81	274.12
Wood	R ²	0.71	0.75	0.75	0.81	0.79	0.81	0.81	0.82	0.71	0.75	0.73	0.79
	AIC	250.71	253.41	244.85	234.38	−89.20	−87.94	−90.20	−85.50	246.50	242.16	242.58	236.32

I, II, III, IV—represents linear, second-order polynomial, factorial regression, and quadratic regression equation, respectively

Bold font means model chosen to further analysis

R²—higher = better

AIC—lower = better

Table A2. Results of regression models of proximate analysis; moisture content (MC), organic matter content (OM), ash content (AC), and combustible parts (CP) of CSF determined from RDF components concerning pyrolysis temperature and residence time.

Material	Assessment Criterion	Models of MC				Models of OM				Models of AC				Models of CP			
		I	II	III	IV	I	II	III	IV	I	II	III	IV	I	II	III	IV
Carton	R ²	0.04	0.06	0.09	0.11	0.68	0.76	0.70	0.78	0.73	0.82	0.76	0.84	0.34	0.82	0.76	0.84
	AIC	425.41	427.25	422.39	424.12	777.69	753.01	773.20	746.24	711.09	678.84	703.21	666.26	711.09	678.84	703.21	666.26
Fabric	R ²	0.12	0.13	0.12	0.13	0.28	0.31	0.28	0.31	0.35	0.35	0.35	0.35	0.35	0.35	0.35	0.35
	AIC	572.20	575.01	573.90	576.71	394.74	394.50	396.29	396.03	248.23	251.34	249.77	252.87	248.23	251.34	249.77	252.87
Kitchen waste	R ²	0.08	0.09	0.09	0.10	0.41	0.42	0.48	0.49	0.34	0.35	0.38	0.40	0.34	0.35	0.38	0.40
	AIC	552.21	555.48	553.32	556.59	779.34	781.83	769.64	771.94	701.54	703.77	696.17	698.26	701.54	703.77	696.17	698.26
Paper	R ²	0.10	0.18	0.12	0.21	0.65	0.67	0.70	0.72	0.57	0.60	0.60	0.63	0.57	0.59	0.60	0.63
	AIC	474.00	468.17	473.05	466.91	835.09	832.68	821.55	818.02	795.10	793.79	789.61	787.88	795.78	794.28	790.13	788.18
Plastic	R ²	0.13	0.32	0.15	0.35	0.36	0.56	0.49	0.69	0.42	0.62	0.57	0.77	0.42	0.62	0.57	0.77
	AIC	228.08	207.06	227.11	205.21	1019.27	986.02	998.46	952.73	906.47	869.28	877.36	819.24	906.47	869.28	877.36	819.24
Rubber	R ²	0.02	0.03	0.04	0.05	0.81	0.83	0.82	0.84	0.76	0.77	0.76	0.78	0.76	0.77	0.76	0.78
	AIC	278.67	281.69	278.24	281.23	795.10	790.14	792.82	787.44	761.22	757.62	761.65	757.92	761.22	757.62	761.65	757.92
PAP/AL/PE composite packaging pack	R ²	0.09	0.49	0.09	0.49	0.72	0.82	0.73	0.83	0.79	0.85	0.79	0.86	0.79	0.85	0.79	0.86
	AIC	440.29	387.26	441.96	388.67	790.44	748.72	790.20	747.14	753.19	719.22	752.86	717.78	753.19	719.22	752.86	717.78
Wood	R ²	0.05	0.05	0.05	0.05	0.44	0.49	0.44	0.49	0.30	0.32	0.31	0.32	0.31	0.32	0.31	0.32
	AIC	526.03	529.91	528.00	531.88	602.39	596.66	604.39	598.66	556.27	558.76	557.84	560.32	556.52	558.97	558.05	560.49

I, II, III, IV—represents linear, second-order polynomial, factorial regression, and quadratic regression equation, respectively

Bold font means model chosen to further analysis

R²—higher = better

AIC—lower = better

Table A3. Results of regression models of ultimate analysis; carbon content (C), hydrogen content (H), nitrogen content (N), and sulfur (S) of CSF determined from RDF components concerning pyrolysis temperature and residence time.

Material	Assessment Criterion	Models of C				Models of H				Models of N				Models of S			
		I	II	III	IV	I	II	III	IV	I	II	III	IV	I	II	III	IV
Carton	R ²	0.28	0.31	0.43	0.46	0.81	0.91	0.82	0.92	0.24	0.33	0.32	0.41	0.19	0.20	0.25	0.26
	AIC	155.21	157.48	149.58	151.40	74.66	53.18	75.56	52.75	6.00	10.00	8.00	12.00	−103.41	−99.50	−103.93	−100.03
Fabric	R ²	0.50	0.59	0.53	0.62	0.69	0.75	0.73	0.79	0.48	0.50	0.49	0.51	0.17	0.38	0.18	0.39
	AIC	250.53	247.93	250.81	247.81	111.48	108.26	109.36	105.06	41.59	44.39	43.32	46.10	−73.76	−79.35	−72.44	−78.26
Kitchen waste	R ²	0.08	0.25	0.10	0.26	0.80	0.83	0.80	0.83	0.40	0.44	0.42	0.46	0.15	0.33	0.17	0.35
	AIC	205.12	202.63	206.69	204.10	62.00	59.98	63.68	61.59	38.23	40.25	39.44	41.40	−127.42	−131.31	−126.36	−130.51
Paper	R ²	0.05	0.08	0.21	0.24	0.79	0.85	0.82	0.88	0.53	0.68	0.54	0.69	0.08	0.43	0.14	0.49
	AIC	174.17	177.10	170.06	172.75	72.24	65.33	69.46	60.55	−134.97	−142.61	−133.25	−141.02	−101.24	−112.91	−101.59	−114.79
Plastic	R ²	0.43	0.55	0.59	0.72	0.39	0.49	0.55	0.66	0.09	0.12	0.10	0.13	0.44	0.64	0.58	0.78
	AIC	283.75	279.63	274.50	266.42	186.60	184.37	178.12	173.23	38.18	41.14	39.94	42.90	−99.17	−109.64	−107.19	−124.84
Rubber	R ²	0.68	0.68	0.68	0.69	0.79	0.90	0.79	0.91	0.26	0.29	0.35	0.38	0.19	0.19	0.26	0.28
	AIC	228.13	231.84	229.86	233.57	71.31	50.69	72.62	47.99	−79.03	−76.19	−80.69	−78.01	−100.17	−96.35	−101.41	−97.92
PAP/AL/PE composite packaging pack	R ²	0.00	0.34	0.30	0.63	0.54	0.67	0.58	0.72	0.17	0.21	0.17	0.21	0.13	0.51	0.24	0.61
	AIC	238.66	229.32	229.18	212.18	132.35	124.97	131.10	122.22	−73.69	−71.25	−71.78	−69.34	−135.93	−150.21	−137.99	−155.79
Wood	R ²	0.63	0.64	0.70	0.72	0.63	0.64	0.70	0.72	0.32	0.35	0.44	0.46	0.07	0.32	0.08	0.33
	AIC	171.08	173.86	166.00	168.49	171.08	173.86	166.00	168.49	−2.69	0.29	−6.17	3.18	−170.48	−176.61	−168.86	−175.00

I, II, III, IV—represent linear, second-order polynomial, factorial regression, and quadratic regression equation, respectively

Bold font means the model chosen to further analysis

R²—higher = better

AIC—lower = better

References

1. Mavropoulos, A. Waste Management 2030+. Available online: <https://waste-management-world.com/a/waste-management> (accessed on 13 December 2020).
2. Sherwood, J. The significance of biomass in a circular economy. *Bioresour. Technol.* **2020**, *300*. [CrossRef]
3. Bagheri, M.; Esfilar, R.; Sina Golchi, M.; Kennedy, C.A. Towards a circular economy: A comprehensive study of higher heat values and emission potential of various municipal solid wastes. *Waste Manag.* **2020**, *101*, 210–221. [CrossRef]
4. Kaczor, Z.; Buliński, Z.; Werle, S. Modelling approaches to waste biomass pyrolysis: A review. *Renew. Energy* **2020**, *159*, 427–443. [CrossRef]
5. Stępień, P.; Pulka, J.; Serowik, M.; Białowiec, A. Thermogravimetric and calorimetric characteristics of alternative fuel in terms of its use in low-temperature pyrolysis. *Waste Biomass Valori.* **2019**, *10*, 1669–1677. [CrossRef]
6. Ayeleru, O.O.; Dlova, S.; Akinribide, O.J.; Ntuli, F.; Kupolati, W.K.; Marina, P.F.; Blencowe, A.; Olubambi, P.A. Challenges of plastic waste generation and management in sub-Saharan Africa: A review. *Waste Manag.* **2020**, *110*, 24–42. [CrossRef]
7. Buczma, S.R. Fighting waste crime: Legal and practical challenges: What lesson has been learned more than ten years after the adoption of Directive 2008/99? *Era Forum* **2020**. [CrossRef]
8. Levoyannis, C. The EU Green Deal and the Impact on the Future of Gas and Gas Infrastructure in the European Union. In *Aspects of the Energy Union: Application and Effects of European Energy Policies in SE Europe and Eastern Mediterranean*; Mathioulakis, M., Ed.; Springer International Publishing: Cham, Switzerland, 2021; pp. 201–224. ISBN 978-3-030-55981-6. [CrossRef]
9. Herrero, M.; Laca, A.; Laca, A.; Díaz, M. Application of life cycle assessment to food industry wastes. *Food Ind. Wastes* **2020**, *331–353*. [CrossRef]
10. Pires, A.; Martinho, G.; Rodrigues, S.; Gomes, M.I. Preparation for Reusing, Recycling, Recovering, and Landfilling: Waste Hierarchy Steps After Waste Collection. In *Sustainable Solid Waste Collection and Management*; Springer International Publishing: Cham, Switzerland, 2019; pp. 45–59. ISBN 978-3-319-93200-2. [CrossRef]
11. Stępień, P.; Serowik, M.; Koziel, J.A.; Białowiec, A. Waste to carbon: Estimating the energy demand for production of carbonized refuse-derived fuel. *Sustainability* **2019**, *11*, 5685. [CrossRef]
12. Białowiec, A.; Pulka, J.; Stępień, P.; Manczarski, P.; Gołaszewski, J. The RDF/SRF torrefaction: An effect of temperature on characterization of the product—Carbonized refuse derived fuel. *Waste Manag.* **2017**, *70*, 91–100. [CrossRef]
13. Jewiarz, M.; Mudryk, K.; Wróbel, M.; Frączek, J.; Dziedzic, K. Parameters affecting RDF-based pellet quality. *Energies* **2020**, *13*, 910. [CrossRef]
14. Świechowski, K.; Syguła, E.; Koziel, J.A.; Stępień, P.; Kugler, S.; Manczarski, P.; Białowiec, A. Low-temperature pyrolysis of municipal solid waste components and refuse-derived fuel—Process efficiency and fuel properties of carbonized solid fuel. *Data* **2020**, *5*, 48. [CrossRef]
15. Świechowski, K.; Stegenta-Dabrowska, S.; Liszewski, M.; Babelewski, P.; Koziel, J.A.; Białowiec, A. Oxytree pruned biomass torrefaction: Process kinetics. *Materials*. **2019**, *12*, 3334. [CrossRef] [PubMed]
16. Stępień, P.; Świechowski, K.; Hnat, M.; Kugler, S.; Stegenta-Dabrowska, S.; Koziel, J.A.; Manczarski, P.; Białowiec, A. Waste to carbon: Biocoal from elephant dung as new cooking fuel. *Energies* **2019**, *12*, 4344. [CrossRef]
17. Syguła, E.; Koziel, J.A.; Białowiec, A. Proof-of-concept of spent mushrooms compost torrefaction—Studying the process kinetics and the influence of temperature and duration on the calorific value of the produced biocoal. *Energies* **2019**, *12*, 3060. [CrossRef]
18. Nobre, C.; Alves, O.; Longo, A.; Vilarinho, C.; Gonçalves, M. Torrefaction and carbonization of refuse derived fuel: Char characterization and evaluation of gaseous and liquid emissions. *Bioresour. Technol.* **2019**, *285*, 121325. [CrossRef]
19. Tripathi, M.; Sahu, J.N.; Ganesan, P. Effect of process parameters on production of biochar from biomass waste through pyrolysis: A review. *Renew. Sustain. Energy Rev.* **2016**, *55*, 467–481. [CrossRef]
20. Lin, J.; Ma, R.; Luo, J.; Sun, S.; Cui, C.; Fang, L.; Huang, H. Microwave pyrolysis of food waste for high-quality syngas production: Positive effects of a CO₂ reaction atmosphere and insights into the intrinsic reaction mechanisms. *Energy Convers. Manag.* **2020**, *206*, 112490. [CrossRef]
21. Wang, L.; Ni, H.; Zhang, J.; Shi, Q.; Zhang, R.; Yu, H.; Li, M. Enzymatic treatment improves fast pyrolysis product selectivity of softwood and hardwood lignin. *Sci. Total Environ.* **2020**, *717*, 137241. [CrossRef]
22. Basu, P. Chapter 2—Biomass Characteristics. In *Biomass Gasification and Pyrolysis*; Basu, P., Ed.; Academic Press: Boston, MA, USA, 2010; pp. 27–63. ISBN 978-0-12-374988-8. [CrossRef]
23. Nunes, L.J.R.; De Oliveira Matias, J.C.; Da Silva Catalão, J.P. Chapter 1—Introduction. In *Torrefaction of Biomass for Energy Applications*; Nunes, L.J.R., De Oliveira Matias, J.C., Da Silva Catalão, J.P., Eds.; Academic Press: Cambridge, MA, USA, 2018; pp. 1–43. ISBN 978-0-12-809462-4. [CrossRef]
24. Municipal Solid Waste. Analysis of Combustible And Non-Combustible Content, PN-Z-15008-04:1993 Standard. Available online: <https://sklep.pkn.pl/pn-z-15008-03-1993p.html> (accessed on 13 December 2020).
25. Waste Characteristics. Determination of Organic Matter Content for Waste, Slurry and Sludge, PN-EN 15169:2011 Standard. Available online: <https://sklep.pkn.pl/pn-en-15169-2011p.html?options=cart> (accessed on 13 December 2020).
26. Determination of the Higher Heating Value and the Lower Heating Value, PN-G-04513:1981 Standard. Solid Fuels. Available online: <https://sklep.pkn.pl/pn-z-15008-04-1993p.html?options=cart> (accessed on 13 December 2020).
27. Caillat, S.; Vakkilainen, E. Large-scale biomass combustion plants: An overview. *Sci. Technol. Eng.* **2013**, 189–224. [CrossRef]

28. Stegenta, S.; Kałdun, B.; Białowiec, A. Model selection and estimation of kinetic parameters of oxygen consumption during biostabilization of under-size fraction of municipal solid waste. *Rocz. Ochr. Środowiska* **2016**, *18*, 800–814. Available online: https://www.researchgate.net/publication/328601322_Model_selection_and_estimation_of_kinetic_parameters_of_oxygen_consumption_during_biostabilization_of_under-size_fraction_of_municipal_solid_waste (accessed on 13 December 2020).
29. Białowiec, A. *Innovations in Waste Management, Selected Issues*; Wydawnictwo Uniwersytetu Przyrodniczego we Wrocławiu: Wrocław, Poland, 2018; ISBN 9788377172780.
30. Özyüğü Uran, A.; Yaman, S. Prediction of Calorific Value of Biomass from Proximate Analysis. *Energy Procedia* **2017**, *107*, 130–136. [[CrossRef](#)]
31. Hosokai, S.; Matsuoka, K.; Kuramoto, K.; Suzuki, Y. Modification of Dulong’s formula to estimate heating value of gas, liquid and solid fuels. *Fuel Process. Technol.* **2016**, *152*, 399–405. [[CrossRef](#)]
32. Demirbas, A.; Ak, N.; Aslan, A.; Sen, N. Calculation of higher heating values of hydrocarbon compounds and fatty acids. *Pet. Sci. Technol.* **2018**, *36*, 712–717. [[CrossRef](#)]
33. Akkaya, E.; Demir, A. Predicting the heating value of municipal solid waste-based materials: An artificial neural network model. *Energy Sources Part A Recover. Util. Environ. Eff.* **2010**, *32*, 1777–1783. [[CrossRef](#)]
34. Tiikma, L.; Tamvelius, H.; Luik, L. Coprocessing of heavy shale oil with polyethylene waste. *J. Anal. Appl. Pyrolysis* **2007**, *79*, 191–195. [[CrossRef](#)]
35. Nobre, C.; Vilarinho, C.; Alves, O.; Mendes, B.; Goncalves, M. Upgrading of refuse derived fuel through torrefaction and carbonization: Evaluation of RDF char fuel properties. *Energy* **2019**, *181*, 66–76. [[CrossRef](#)]
36. Hanif, M.U.; Capareda, S.C.; Iqbal, H.; Arazo, R.O.; Anwar Baig, M. Effects of pyrolysis temperature on product yields and energy recovery from co-feeding of cotton gin trash, cow manure, and microalgae: A simulation study. *PLoS ONE* **2016**, e0152230. [[CrossRef](#)]
37. Liu, Z.; Han, G. Production of solid fuel biochar from waste biomass by low temperature pyrolysis. *Fuel* **2015**, *158*, 159–165. [[CrossRef](#)]
38. Haykiri, H.; Kurt, G.; Yaman, S. Properties of biochars obtained from RDF by carbonization: Influences of devolatilization severity. *Waste Biomass Valorization* **2017**, *8*, 539–547. [[CrossRef](#)]
39. Huo, H.; Ma, Y. TG/DTA—FTIR study on total resource recovery from Tetra Pak waste by pyrolysis under a CO₂ environment. *Prog. React. Kinet. Mech.* **2018**, *43*, 229–235. [[CrossRef](#)]
40. Hunt, J.; Ferrari, A.; Lita, A.; Crosswhite, M.; Ashley, B.; Stiegman, A.E. Microwave-specific enhancement of the carbon–carbon dioxide (Boudouard) reaction. *J. Phys. Chem.* **2013**, *117*, 26871–26880. [[CrossRef](#)]
41. Muley, P.D.; Henkel, C.; Abdollahi, K.K.; Marculescu, C.; Boldor, D. A critical comparison of pyrolysis of cellulose, lignin, and pine sawdust using an induction heating reactor. *Energy Convers. Manag.* **2016**, *117*, 273–280. [[CrossRef](#)]
42. Mui, E.L.K.; Cheung, W.H.; McKay, G. Tyre char preparation from waste tyre rubber for dye removal from effluents. *J. Hazard. Mater.* **2010**, *175*, 151–158. [[CrossRef](#)]
43. Acosta, R.; Tavera, C.; Gauthier-Maradei, P.; Nabarlantz, D. Production of oil and char by intermediate pyrolysis of scrap tyres: Influence on yield and product characteristics. *Int. J. Chem. React. Eng.* **2015**, *13*, 189–200. [[CrossRef](#)]
44. Zeng, K.; Pham Minh, D.; Gauthier, D.; Weiss-Hortala, E.; Nzihou, A.; Flamant, G. The effect of temperature and heating rate on char properties obtained from solar pyrolysis of beech wood. *Bioresour. Technol.* **2015**, *182*, 114–119. [[CrossRef](#)] [[PubMed](#)]
45. Ho Kim, K.; Kim, J.; Cho, T.; Weon Choi, J. Influence of pyrolysis temperature on physicochemical properties of biochar obtained from the fast pyrolysis of pitch pine (*Pinus rigida*). *Bioresour. Technol.* **2012**, *118*, 158–162. [[CrossRef](#)]
46. Zhang, C.; Ho, S.; Chen, W.; Xie, Y.; Liu, Z.; Chang, J.-S. Torrefaction performance and energy usage of biomass wastes and their correlations with torrefaction severity index. *Appl. Energy* **2018**, *220*, 598–604. [[CrossRef](#)]